International Research Journal of Pure and Applied Physics, 12 (1),41-77, 2025
ISSN 2055-009X(Print)
ISSN 2055-0103(Online)
Website: https://www.eajournals.org/
Publication of the European Centre for Research Training and Development -UK

Time-Lapse Geological Assessment of Groundwater and Soil; A Case Study of Oghara Farmlands, Delta State, Nigeria

[1]Ozobeme Azubike Anslem, [2]Osisanya Olajuwon Wasiu, [3]Airen Osariere John, [4]Ibitoye Taiwo Abel, [5]Saleh A. Saleh
[1,3]Department of Physics, University of Benin, Benin City, Edo State.
[2]Department of Physics, College of Science, Federal University of Petroleum Resources, Effurun, Delta State.
[4,5]Department of Petroleum Engineering and Geosciences, Petroleum Training Institute, Effurun, Delta State

doi: https://doi.org/10.37745/irjpap.13vol12n14177 Published December 30, 2025

Citation: Anslem O.A., Wasiu O.O., John A.O., Abel I.T., Saleh S.A. (2025) Time-Lapse Geological Assessment of Groundwater and Soil; A Case Study of Oghara Farmlands, Delta State, Nigeria, *International Research Journal of Pure and Applied Physics*, 12 (1),41-77

Abstract: *The use of mineral fertilizers and nutrients is widely adopted in conventional agricultural practices, playing an essential role in maintaining optimal crop yields and improving overall quality. To aid farmers in effective fertilization and crop management strategies, non-invasive geophysical techniques can offer insights into the nutrient distribution within the soil. This study deemed it imperative to assess the physicochemical parameters and heavy metals (HM) present in the groundwater and soil of the study area. A total of three groundwater samples and five soil samples were collected and tested for different physical properties, such as pH, alkalinity, electrical conductivity (EC), temperature, total hardness (TH), total dissolved solids (TDS), total suspended solids (TSS), dissolved oxygen (DO), biochemical oxygen demand (BOD), chemical oxygen demand (COD), calcium (Ca), magnesium (Mg), sodium (Na), potassium (K), chloride (Cl^-), nitrate (NO_3^-), sulfate (SO_4^{2-}), phosphate (PO_{24}^-), and ammoniacal nitrogen (NH_4–N). The heavy metals (HM) checked included iron (Fe), chromium (Cr), lead (Pb), copper (Cu), zinc (Zn), nickel (Ni), manganese (Mn), and cadmium (Cd). Recently, electrical resistivity tomography (ERT) has been used in local studies to measure changes in soil properties. Unfortunately, the signals we measure from the ground are mixed up because of changes in the soil both sideways and up and down, making it hard to figure out what each change is contributing. The analysis of groundwater and soil revealed that, with the exception of a few parameters, groundwater samples fell below the WHO permissible limit. The soil's porosity, permeability, and the surrounding topography influence the migration rate. The rates of migration vary between the first and second locations.*

International Research Journal of Pure and Applied Physics, 12 (1),41-77, 2025
ISSN 2055-009X(Print)
ISSN 2055-0103(Online)
Website: https://www.eajournals.org/
Publication of the European Centre for Research Training and Development -UK

It has been found that if the vertical migration rate in the dry sand layer (which is about 13.7 meters thick based on drilling data) stays the same, the fertilizer contaminant will take about 0.5 years to reach the wet sandy layer below it in the first location, while in the second location, it will take around 1 year. Detailed calculations to determine the arrival time at the sandy layer has been conducted. Ultimately, it is imperative for the government to guarantee the installation of water purification plants during the process of borehole drilling, as this will help further decrease the existing salinity levels in the groundwater.

Keywords: migration, date, heavy metal, pH, fertilizer, permissible

INTRODUCTION

In conventional agriculture, the application of mineral fertilizers and nutrients is a standard practice essential for achieving optimal yields and high-quality crops. Among these, nitrogen stands out as the most frequently utilized fertilizer; however, its excessive use can result in negative consequences for the environment. To aid farmers in effective fertilization and crop management, non-invasive geophysical techniques can offer insights into the spatial and temporal nutrient distribution within the soil. Agriculture is recognized as a significant contributor to water pollution; however, its geographical characteristics make it particularly challenging to eliminate this issue (Eyankware et al., 2020a; Eyankware and Obasi, 2021). In the study area, the primary agricultural establishment is the palm oil plantation. The prevalence of groundwater pollution, attributed to intensive agricultural activities, stems from the extensive use of fertilizers in farming practices. Eyankware et al. (2022) have documented the effects of these practices on groundwater contamination. Across various regions of the world, there is a significant reliance on chemical fertilizers (Yang et al., 2006) to boost agricultural productivity. This applies applies to palm oil plantations as well, where fertilization occurs bi-monthly with fertilizers containing diverse chemical compositions (as noted in a personal discussion with the farming supervisor). At the start of the year, a total of 400 kg of urea containing 60% nitrogen is applied to a two-hectare palm oil plantation. Following this application, after a span of two months, a supplementary fertilizer comprising 15% nitrogen, 30% phosphorus, and 55% potassium (NPK) is utilized to enhance palm production further. This fertilization cycle is repeated in the middle of the year and persists until the year concludes. Overall, a minimum of 800 kg of urea is utilized annually for fertilizing palm trees across the two-hectare area. The leaching of contaminants, particularly nitrates, from agricultural soils has been extensively researched (Saadi and Maslouhi, 2003; Eyankware et al., 2020; Eyankware et al., 2022). Human activities, such as applying chemical fertilizers in agricultural practices, contribute to nitrate emissions that infiltrate groundwater (Mahvi et al., 2005; Atafare et al., 2010). Research by Islami et al. (2010b) in Kelantan looked into how nitrates contaminate shallow aquifers using a mix of methods, including geoelectrical, hydrogeochemical, and soil property analyses. Their findings indicated that areas characterized by intense fertilization activities exhibited comparatively higher nitrate concentrations. Furthermore, Islami (2010a)

noted that the geoelectrical resistivity measurements at the surface level in fertilized regions were significantly lower than those in non-fertilized counterparts. When hazardous and harmful substances seep into the earth's subsurface, they contaminate groundwater aquifers, endangering the quality and safety of the water that is eventually stored beneath the surface and made available for human consumption and possibly all other areas of human activity that require water. This phenomenon is known as groundwater pollution (GWP). Additionally, Islami (2010a) pointed out that leftover nitrate and chloride from long-term urea use affect the geoelectrical resistivity measurements in those areas. Obire et al. (2008) also demonstrated that the application of fertilizers adversely affects groundwater quality. Alongside subsurface investigations, several groundbreaking studies utilizing the geoelectrical resistivity imaging technique have been conducted by Barker (1981), Akisnseye et al. (2023), Griffiths et al. (1990), Noel and Walker (1990), and Griffiths and Barker (1993). The effectiveness of this technique in addressing various geo-environmental issues has been demonstrated through numerous case studies by Reynolds (1997), Loke (1999), Abdul Nassir et al. (2000), and Baharuddin et al. (2009). Nevertheless, there has been no research focused on the use of geoelectrical resistivity imaging for monitoring chemical fertilizers in agricultural settings characterized by specific soil conditions. Furthermore, it is uncommon for geoelectrical imaging surveys to be paid with laboratory analyses of soil water samples collected from the study site, which would enhance the interpretation of field data. This paper mainly aims to observe how the amounts of chemical fertilizers change over time in the area just below the surface, using methods like geoelectrical resistivity and hydrogeochemical measurements, along with studying soil properties. Additionally, the relationship between fertilizer concentrations in pore soil and geoelectrical resistivity readings was examined, alongside an exploration of nitrate leaching and its dynamics within the sandy soil's vadose zone. Monitoring chemical fertilizers in agricultural regions is crucial, given that the primary water supply in these areas is derived from shallow groundwater accessed through conventional wells.

Location, accessibility, climate and topography

Oghara, in Delta State (Fig. 1), Nigeria, is characterized by a tropical climate that encompasses two prominent seasons: the dry season and the rainy season. Oghara is characterized by consistently high levels of rainfall, averaging approximately 266.5 cm annually, along with a mean temperature ranging from 24°C (75.2°F) to 27°C (80.4°F) throughout the year. The region experiences two primary seasons: the dry season and the rainy season. The dry season spans from November to February, while the principal rainy season lasts from February to October. July sees the heaviest rainfall, and no month is entirely devoid of rain; January typically receives up to 2.5 cm of precipitation (Aweto and Igben, 2003). The 'harmattan,' which brings cool, dry, and dusty conditions, marks the weather from December to February. Furthermore, the diurnal temperature variation is minimal, with seasonal temperature fluctuations of approximately 25°C (82°F) during the rainy season and 28°C (82°F) in the dry season. The relative humidity in the area ranges from 60 to90 percent (Udo, 1970).

Geology of the study area/Hydrogeology

The local geological area exhibits three primary depositional (sedimentary) environments: marine, mixed, and continental. Utilizing the classification of sedimentary environments, the sedimentary sequence is characterized by three distinct rock formations: Benin, Agbada, and Akata. In the oil-producing communities of the Niger Delta, the source and seal rocks comprise the marine/deltaic, plastic, and over-pressured shales found within the Akata and Agbada formations. The geological composition of the study area reveals an array of materials, including clay, sand, pebbles, sandstone, gravel, shales, mangrove swamps, lignite, and alluvium. The hydrogeological characteristics of the research area are defined by a multifaceted aquifer system that exhibits diverse groundwater quality and varying degrees of vulnerability. Investigations conducted within this region have primarily aimed at elucidating aspects of groundwater quality, the direction of flow, and the elements that influence the vulnerability of the aquifers (Oseji, et al., 2020).

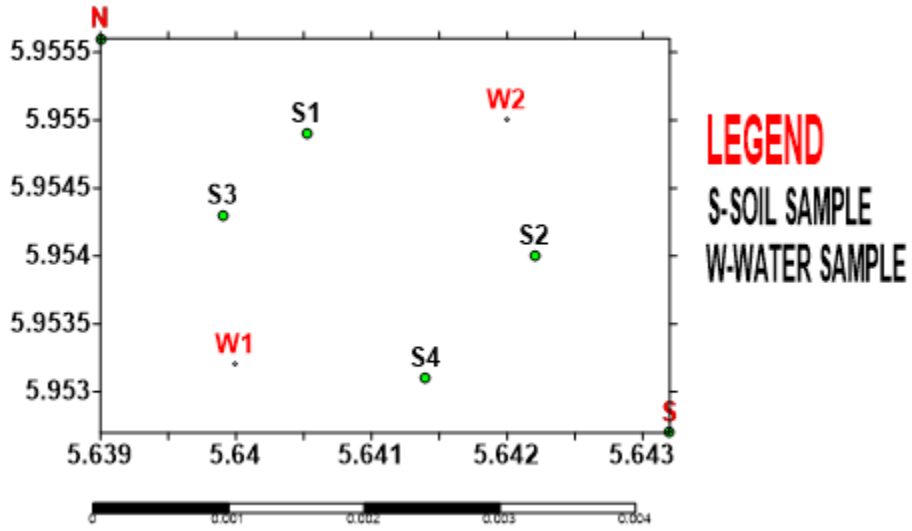

Fig. 1: Base Map of the study area

METHODOLOGY

Two-dimensional (2D) resistivity imaging

The 2D resistivity survey was executed with the use of the PASI Terrameter. Data measurements were taken in sequences at intervals of 10 m, 20 m, 30 m, 40 m, 50 m, and 60 m, employing four (4) electrodes across all traverses, each covering a length of 200 m. The apparent resistivity values for each traverse were organized into a format compatible with the RES2DINV inversion software. Since the surveyed region was relatively flat, elevation corrections were omitted from the measurements. The inversion of the 2D data was performed using the RES2DINV code (Loke and Barker 1996a). For the forward modeling subroutine that computes apparent resistivity values, a

grid configuration of 4 nodes per unit electrode along with a normal mesh was employed. The initial and minimum damping factors set for the inversion were 0.225 and 0.05, respectively, contrasting with the default values of 0.160 and 0.015. To account for the exponential decrease in resistivity resolution with depth, the damping factor was permitted to increase by a factor of 1.05 as depth increased. This optimization of the damping factor aimed to considerably decrease the number of iterations needed for convergence, although it resulted in an increase in the time required for each iteration. The complete set of 2D lines, consisting of 10 traverses for both the Erhoike Community and Okpare Community, was integrated to create a unified 3D data set. This integration involved converting the recorded 2D data (apparent resistivity values) into a 3D format compatible with the RES3DINV software (Loke and Barker 1996b) through the utilization of the RES2DINV computer program. To achieve this, the coordinates, line orientations, quantity of electrodes, electrode spacing, and data levels for each of the 2D traverses were employed to compile the apparent resistivity values, assisted by an input text file that the computer code could interpret. The gathered 3D data sets were processed using the RES3DINV software, which automatically generates a 3D model representing the distribution of resistivity based on apparent resistivity measurements acquired from a 3D resistivity imaging survey (Li and Oldenburg 1994; White et al. 2001). For optimal results, the electrodes utilized in such surveys are typically organized in square grids. The inversion technique implemented in the RES3DINV program relies on the smoothness constrained least-squares approach (de Groot-Hedlin and Constable 1990; Sasaki 1992), similar to the method used in RES2DINV for two-dimensional inversions, although a robust inversion can also be performed. This program provides users the flexibility to modify the damping factor and flatness filters within the aforementioned equation to align with the specifics of the data set undergoing inversion. An initial damping factor of 0.215 was employed to invert the assembled 3D apparent resistivity dataset. Following each iteration, the inversion subroutine typically lowered the damping factor applied; a minimum threshold (set at one-tenth of the initial damping factor) was established to ensure the stability of the inversion process. The optimization of the damping factor aimed to minimize the number of iterations needed for the program to achieve convergence by identifying the ideal damping factor that results in the smallest RMS error; however, this optimization consequently lengthens the duration of each iteration. To ascertain the 3D distribution of the model resistivity values based on the apparent resistivity values, the subsurface was divided into several small square blocks. The program established the thickness of the first layer according to the maximum depth of the array's investigation, which was then increased by 1.15 (15%) for the subsequent layers. Finite difference grids consisting of three nodes between neighboring electrodes were employed. A homogeneous earth model served as the initial model for the conducted inversion.

Groundwater Samples Collection

Water samples from three (3) designated sampling points within the study area were collected. Two (2) of these samples were taken from the impacted zone, while one (1) sample was sourced from a control site situated away from the affected region. Each sample was contained in a one-liter clean plastic bottle and securely sealed. The locations of Well (W1) at PRESCO farmland and Well (W2) at UGBEKUN farmland were recorded utilizing a Global Positioning System (GPS).

Furthermore, a sample was also obtained from a borehole that extends 45 meters deep across the northern, northwestern, and southwestern parts of the area, as depicted in Fig. ****. The sole physical characteristic evaluated in the field was the water's color. The collected samples were directly forwarded to the laboratory for analysis without preservation. Prior to conducting the analysis, the water samples were filtered to remove any suspended particles.

Soil Sampling

Soil samples were obtained from five (5) distinct sites within the two specified study areas using a soil auger. A steel auger was utilized to extract soil samples from depths of 0 to 15 cm, which were then placed into clear plastic bags for storage. Upon arrival at the laboratory, these samples were air-dried over several days by spreading them on transparent plastic sheets laid out on a workbench. Sampling occurred at varying depths of 0 to 10 cm, 10 to 25 cm, and 25 to 30 cm, respectively. The surface soil was removed to a depth of 15 cm, followed by the extraction of the subsurface soil; this method was uniformly applied to all additional sampling sites. A mechanical shaker was utilized to thoroughly mix the flasks for at least 30 minutes. Subsequently, the resultant materials were filtered through ashless Whatman filter paper 40 and gathered into 100 cm^3 plastic containers. The control samples underwent initial analysis to determine background target analytes before being spiked with specified concentrations of heavy metals. Following this, a comprehensive extraction procedure was performed to assess the recovery rates. The percent recoveries were calculated by comparing the initial baseline concentrations with those of the spiked samples. For the purpose of spiking the samples with cadmium, cadmium nitrate was prepared as a versatile reagent, ensuring a minimum purity of 99 percent. cadmium nitrate was prepared as a versatile reagent, ensuring a minimum purity of 99 percent. To create solutions for spiking samples with lead, copper, and zinc, analytical-grade lead nitrate, along with analytical-grade granules of copper and zinc, were employed. A reagent blank was prepared for each metal and underwent the full procedural protocol before being utilized for sample analysis. Calibration curves were generated using analytical-grade metals and their respective metal salts. The concentrations of cadmium, copper, lead, and zinc were assessed using a Varian Techtron AA6 atomic absorption spectrophotometer, paired with the appropriate metallic hollow cathode lamps. Acetylene gas functioned as the fuel source, complemented by air as the supporting medium. An oxidizing flame was consistently applied throughout the process. The concentrations of the four metals were obtained through calibration curves. For instrument calibration, a reagent blank was introduced. Following this, standard solutions were aspirated, and extracts from soil samples were subsequently analyzed.

RESULTS AND DISCUSSION

International Research Journal of Pure and Applied Physics, 12 (1),41-77, 2025
ISSN 2055-009X(Print)
ISSN 2055-0103(Online)
Website: https://www.eajournals.org/
Publication of the European Centre for Research Training and Development -UK

Table 1 : Results of physicochemical/heavy metal in groundwater at Presco Low Land and Upland Water Samples

Parameters	pH	EC	TDS	TSS	DO	BOD	COD	Total hardness	Alkalinity	Temp.	Ca	Mg	Na	K	Cl	NO_3^-	SO_4^{2-}	PO_4^-	NH4-N	Fe	Cr	Pb	Cu	Zn	Ni	Mn	Cd
Units	NA	µs/cm	mg/1	mg/1	mg/1	mg/I	mg/I	mg/I	mg/I	NA	mg/I	mg/I	mg/I	mo/!	mg/I	mg/!	mg/I	mg/!	mg/1	mg/I	mg/I	mg/I	mg/I	mg/I	mg/I	mg/I	mg/1
Sample 1	5.53	12	6.3	<0.001	8.2	4	24.4	13	30.8	30.1	6.5	8.3	7.1	10.6	16.4	1.72	0.87	0.75	1.64	0.06	0.008	ND	0.02	0.04	<0.005	0.013	ND
Sample 2	5.74	57	23.8	<0.001	6	2.8	20.7	16.7	42	29.4	10.6	12.2	10.4	14.9	20.9	1.25	1.14	1.08	2.04	0.14	0.021	<0.005	0.05	0.08	<0.005	0.022	ND
Control	6.83	40	20	<0.001	12.4	6.2	32.8	9.1	22.7	28.6	4.7	5.8	5.4	8.3	9.4	0.68	0.82	0.21	0.07	0.02	<0.005	ND	0.011	0.014	ND	ND	ND
min.	5.53	12	6.3	0	6	2.8	20.7	9.1	22.7	28.6	4.7	5.8	5.4	8.3	9.4	0.68	0.82	0.21	0.07	0.02	0.008	0	0.011	0.014	0	0.013	0
max.	6.83	57	23.8	0	12.4	6.2	32.8	16.7	42	30.1	10.6	12.2	10.4	14.9	20.9	1.72	1.14	1.08	2.04	0.14	0.021	0	0.05	0.08	0	0.022	0
aver.	6.03	36.33	16.7	0	8.87	4.33	25.97	12.93	31.83	29.37	7.27	8.77	7.63	11.27	15.57	1.22	0.94	0.68	1.25	0.07	0.01	0	0.03	0.05	0	0.02	0

Table 2: Results of physicochemical/heavy metal in soil at Presco Low Land and Upland Soil Samples

Parameters		pH	EC	ALKALINITY	Ca	Mg	Na	K	Cl^-	NO_3^-	SO_4^{2-}	Fe	Cr	Pb	Cu	Zn	Ni	Cd	Mn
SITE1	SAMPLE 1	6.24	165	60.4	114	121.8	53.6	56	38.2	3.26	4.8	123.8	18.6	8.7	34.5	439	5.77	2.1	5.92
	SAMPLE 2	6.65	130	73.7	103.6	110.9	48.2	50.5	29.5	1.85	3.77	117.9	13	6.4	27.7	36	4.92	1.82	4.77
SITE2	SAMPLE 1	5.34	142	52	88.7	92.5	33.6	35.7	26.7	2.55	1.48	90.5	9.06	5.7	20.1	24.9	3.54	0.95	4.32
	SAMPLE 2	5.28	101	50.6	76	53	38.2	40.1	23.8	2.63	1.35	76.7	6.12	3.8	16.7	12.3	3.08	0.68	2.8
CONTROL		7.2	158	48	90.4	44.7	20	23.8	32.1	0.82	0.75	38.2	2.88	ND	3.8	4.1	<0.005	ND	<0.005
Min		5.28	101	48	76	44.7	20	23.8	23.8	0.82	0.75	38.2	2.88	3.8	3.8	4.1	3.08	0.68	2.8
Max		7.2	165	73.7	114	121.8	53.6	56	38.2	3.26	4.8	123.8	18.6	8.7	34.5	43.9	5.77	2.1	5.92
Aver.		6.17	137.42857	58.057143	94.671429	84.2	38.171429	40.842857	30.328571	2.17	2.5285714	87.014286	10.162857	6.1833333	20.157143	24.17	4.36	1.38	4.4216667

Note as soil unit of parameters are in mk/kg, except for pH, EC, and Alkalinity,

International Research Journal of Pure and Applied Physics, 12 (1),41-77, 2025
ISSN 2055-009X(Print)
ISSN 2055-0103(Online)
Website: https://www.eajournals.org/
Publication of the European Centre for Research Training and Development -UK

DISCUSSION

Assessment of physicochemical parameters in groundwater

pH

According to Eyankware et al. (2020b), the term pH is globally recognized as a measure of the acidity or alkalinity of a solution. Rao and Rao (1991) noted that pH does not directly impact humans; rather, variations in pH levels affect all biochemical reactions. In the study area, the pH values fluctuate between 5.53 and 6.83, with an average value of 6.03 as detailed in Table 1. The fluctuations in pH levels observed in the groundwater samples examined could be attributed to the characteristics of the aquifer, as well as geological factors and seasonal changes (Chanderaseker et al. 2013; Adeyeye et al. 2021). The concentration of pH for this study is below the threshold value of pH in groundwater.

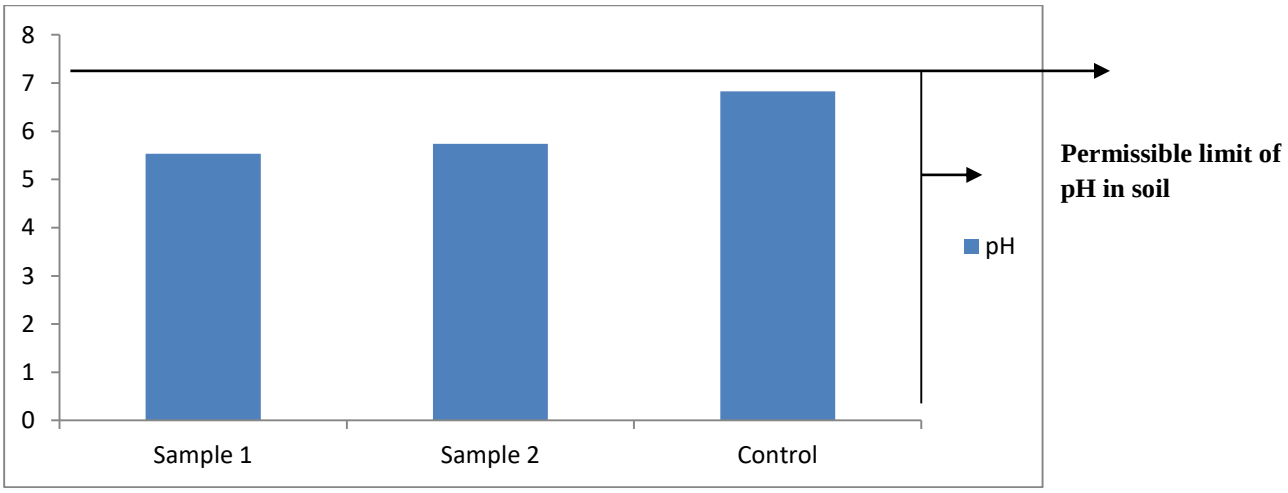

Fig. 2: Plot of pH against sampling points

Electrical conductivity

The main contributor to electrical conductivity in water is the existence of dissolved ions, which are particles that possess an electric charge (Onwe, et al., 2022). For instance, in saltwater, ions such as sodium and chloride are present and can move freely, facilitating the flow of electric current through the water. Conversely, pure water exhibits very low conductivity due to its minimal concentration of dissolved ions. EC ranges from 12 to 57µs/cm, with an average value of 36.33 µs/cm. Deduction from the study suggested that the concentration of EC is below WHO threshold value of 1000 µs/cm, hence the water is considered suitable for drinking purpose.

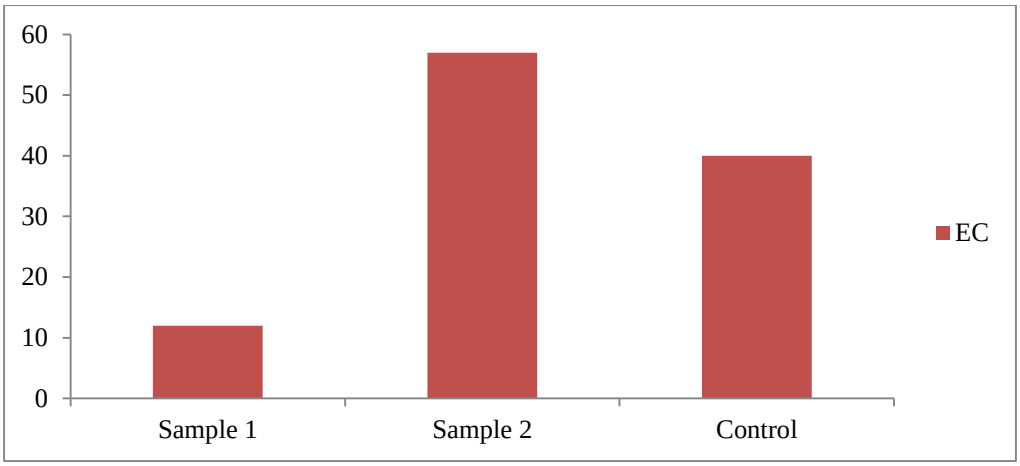

Fig. 3: Plot of EC against sampling points

Total Dissolved Solid (TDS)

TDS present in water originate from numerous sources, encompassing both natural and anthropogenic factors. Natural origins consist of minerals leached from geological formations and soil, whereas human activities, such as sewage discharge, urban runoff, industrial effluents, and the application of de-icing agents on roads, significantly add to the levels of TDS. From Table 1, and Fig. 4 TDS for this study ranges from 6.5 to 23.8 mg/L with average value of 16.17mg/L. The concentration of TDS in groundwater is below the permissible limit of 500 mg/L for NSDWQ, and WHO, (2011)

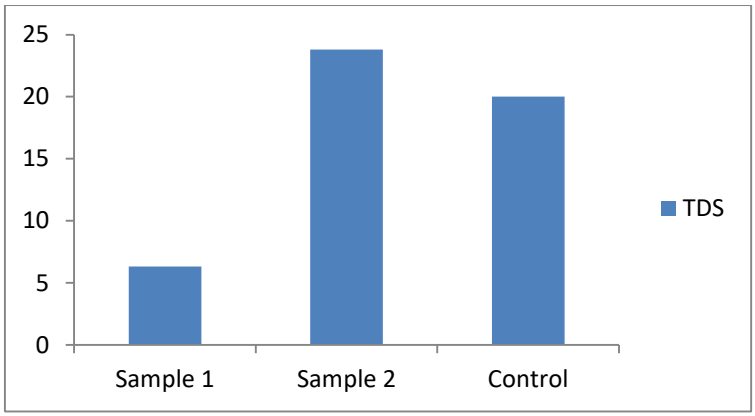

Fig. 4: Plot of TDS against sampling points

Total Suspended Solids (TSS)

The concentration of TSS for this study is less than 0.001, hence considered to be below permissible limit for WHO, 2011.TSS present in water can stem from numerous natural and anthropogenic sources. Natural contributors consist of erosion, runoff from storms, and the proliferation of algae. Conversely, human-related sources are often linked to specific industries,

including manufacturing, food processing, and leachate from landfills. Finding from Table 1, sh0wed TSS values were below zero

Dissolved oxygen (DO)

DO present in water originates from two main sources: the atmosphere and the process of photosynthesis. Oxygen enters the water primarily through diffusion from the atmosphere, which is facilitated by surface disturbances and turbulence. Additionally, aquatic vegetation contributes to the oxygen levels in water by releasing it as a byproduct of photosynthetic activity. The concentration of DO ranges from 6 to 12.4 mg/L, with an average value of 8.87mg/L see Table 1, and Fig. 5. There is no definitive "permissible limit" for dissolved oxygen (DO) in drinking water; instead, there exists an ideal range that supports both healthy water quality and the sustainability of aquatic organisms. Typically, DO concentrations in drinking water should exceed 6.5-8 mg/L, corresponding to a saturation level of 80-120%. A threshold of 4-6 mg/L is frequently regarded as essential for the well-being of aquatic life. Elevated DO levels are usually favored, as they reflect superior water quality.

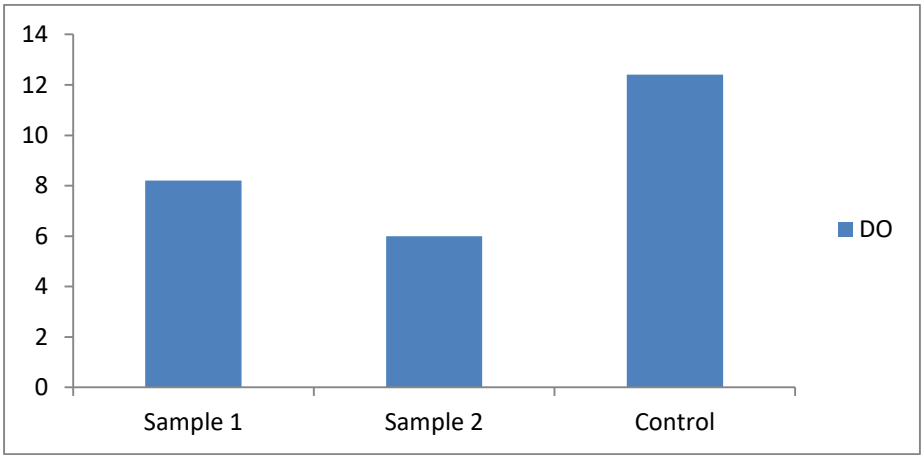

Fig. 5: Plot of DO against sampling points

Biochemical Oxygen Demand (BOD)

BOD in drinking water can be traced back to a variety of sources, encompassing both natural and anthropogenic factors. Among the natural contributors are decomposing organic materials, including foliage, deceased vegetation, and animal remains. Additionally, human-related activities, such as the runoff from industrial and agricultural processes, the release of wastewater, and malfunctioning septic systems, play a significant role in elevating BOD levels. The acceptable threshold for Biochemical Oxygen Demand (BOD) in potable water is typically regarded as being below 5.0 mg/L. At this concentration, BOD is deemed safe and does not adversely affect human health. Conversely, water exhibiting BOD levels greater than 6 mg/L is frequently classified as contaminated and necessitates corrective measures. The concentration of BOD for this study ranges from 2.8 to 6.2 mg/L, with an average value 4.33 mg/L as shown in Table 1 and Fig. 6.

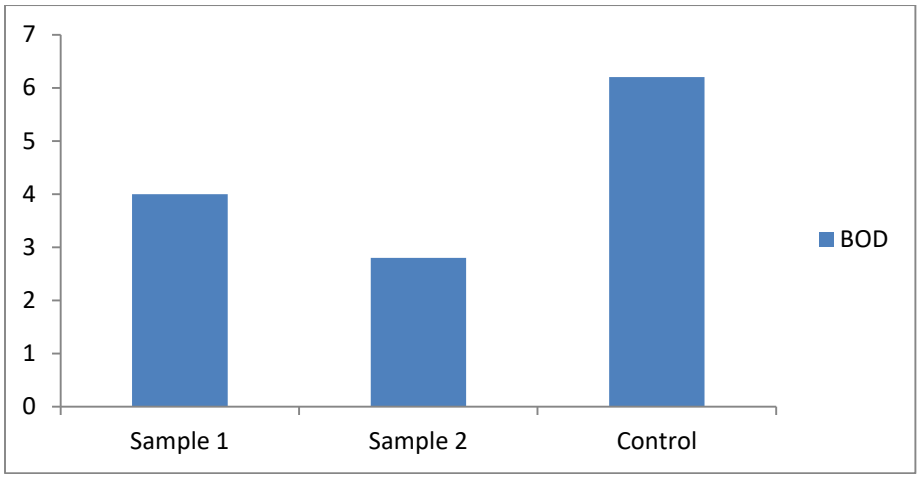

Fig. 6: Plot of BOD against sampling points

Chemical Oxygen Demand (COD)

COD in the context of drinking water pertains to the quantity of oxygen required for the chemical oxidation of all organic materials found within a water sample. This metric serves as an indicator of the water's potential to deplete oxygen levels, driven by the presence of oxidizable organic matter. Although COD is not a definitive gauge of the safety of drinking water, elevated COD levels can suggest the existence of organic contaminants, which may adversely impact the quality of the water. The acceptable threshold for COD in potable water is typically regarded as being below 3 mg/L. However, certain references propose a maximum level of 4 ppm (mg/L). Elevated COD readings may signal the presence of organic contamination, necessitating additional treatment measures or the exploration of alternative water supplies. The concentration of BOD for this study ranges from 20.7 to 32.8 mg/L, with an average value 25.7 mg/Las shown in Table 2, and Fig.6.

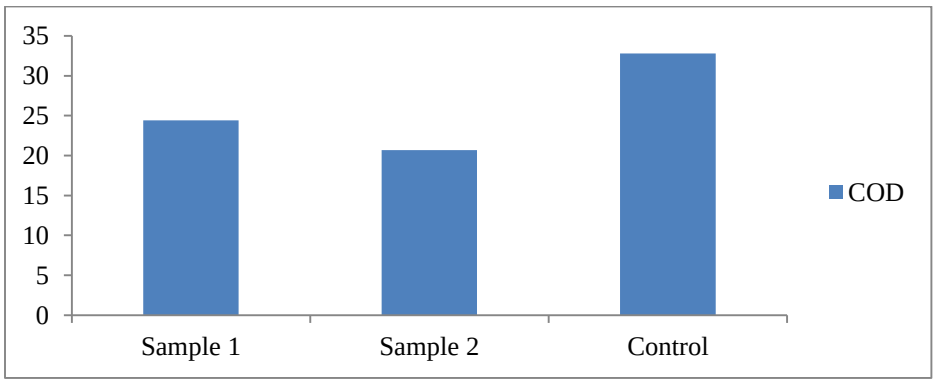

Fig. 7: Plot of COD against sampling points

Total Hardness (TH)

The primary contributors to TH in drinking water are the dissolved ions of calcium and magnesium, which enter the water as it percolates through soil and rock formations rich in these minerals. Notably, limestone and chalk are significant sources of these minerals. Additionally, there are other less significant contributors such as aluminum, barium, iron, manganese, strontium, and zinc. The concentration of TH in groundwater for this study, ranges from 9.1 to 16.7 mg/L, with an average value of 12.93 mg/L as shown in Table 1 and Fig. 8. Findings suggested that the concentration of TH for this study is below the permissible limit of 500mg/L for NSDWQ, and WHO, (2011)

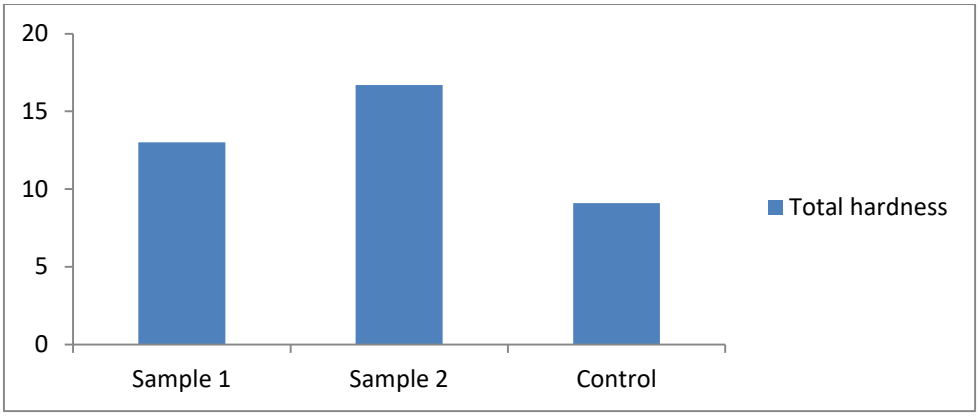

Fig. 8: Plot of TH against sampling points

Alkalinity

The concentration of alkalinity for this study ranges from 22.7 to 42 mg/L, with an average value of 31.83 mg/L see Table 1, and Fig. 9. The alkalinity of drinking water largely arises from the existence of bicarbonates, carbonates, and, on occasion, hydroxides. These ions play a crucial role in enabling the water to neutralize acids and sustain a consistent pH level. Typically, these compounds are naturally occurring in water sources as it engages with rocks and soils that contain carbonate, bicarbonate, and hydroxide materials. According to IS 10500:2012, the acceptable threshold for alkalinity in drinking water is set at 600 mg/L expressed as CaCO3. In contrast, the recommended level should be maintained below 200 mg/L. Findings from the study revealed that alkalinity is below permissible limit.

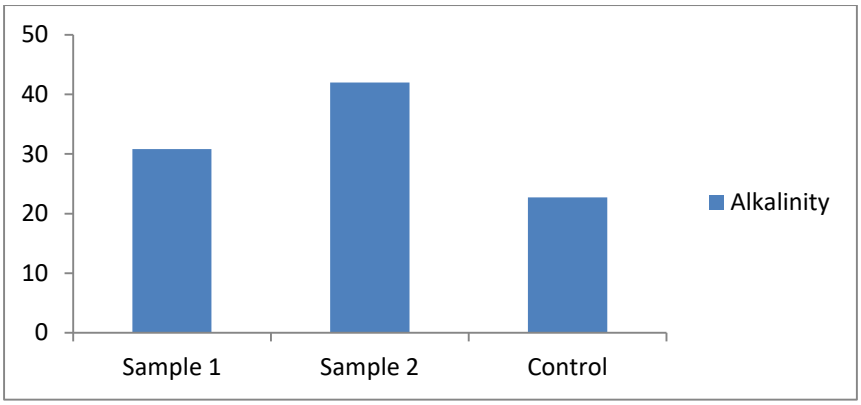

Fig. 9: Plot of Alkalinity against sampling points**.**

Temperature

The temperature of water plays a crucial role as a vital quality within environmental parameters. Accurately measuring water temperature is essential, as it allows us to assess various characteristics of the water, including its chemical, biological, and physical properties, along with any potential health implications. Moreover, water temperature significantly impacts the determination of a water body's suitability for human consumption and use. The temperature of soil for this study ranges from 28.6 to 30.1°C, with an average value of 29.37°C see Table 1, and Fig. 10.

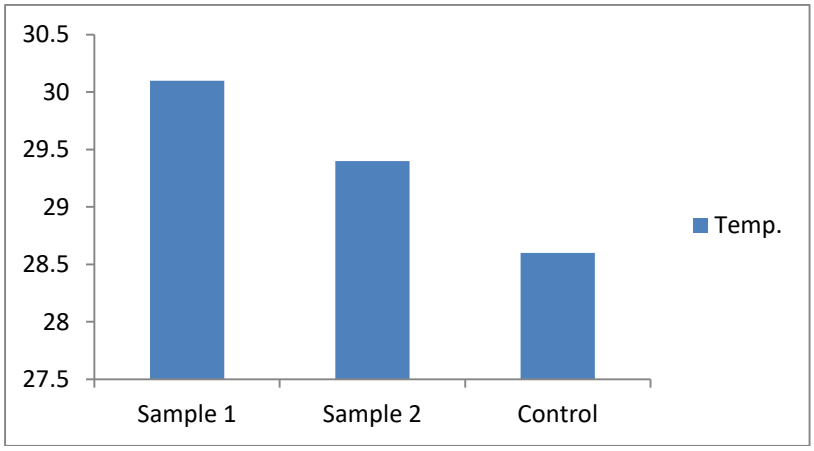

Fig. 10: Plot of temperature against sampling points**.**

Calcium (Ca)

The concentration of Ca in soil ranges from 4.7 to 10.6 mg/L, with an average value of 8.37mg/L see Table 1 and Fig. 11. Ca value for this study is below the permissible limit of 75 mg/L recommended by WHO, (2011). Calcium naturally finds its way into drinking water through the dissolution of rocks that are rich in calcium, such as limestone, as water seeps through the soil and geological formations (Eyankware, et al., 2014). This phenomenon is an inherent aspect of the

water cycle and contributes to the formation of hard water, characterized by elevated levels of dissolved calcium.

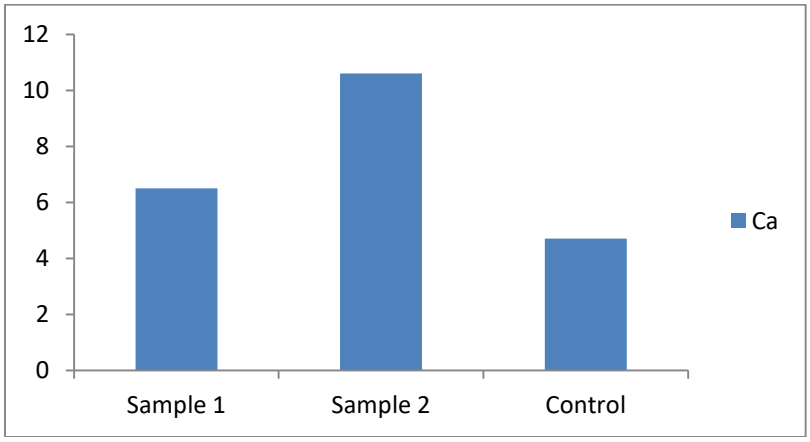

Fig. 11: Plot of Ca against sampling points**.**

Magnesium (Mg)

The presence of magnesium in drinking water is predominantly attributed to the dissolution of minerals found in the earth's crust, which subsequently enter various water sources. Notably, ferromagnesian minerals and magnesium carbonates within rocks play a significant role in imparting hardness to the water. Furthermore, magnesium may be found in tap, mineral, and bottled water; however, the levels of concentration can differ considerably based on the specific source and brand. For this study, the concentration of Mg ranges from 5.8 to 12.2mg/L, with an average value of 8.77mg/L as shown in Table 1, and Fig. 12. The concentration of Mg for this study is below the permissible limit of 250 mg/L recommended by WHO, (2011). Based on the finding groundwater is considered suitable for drinking purpose.

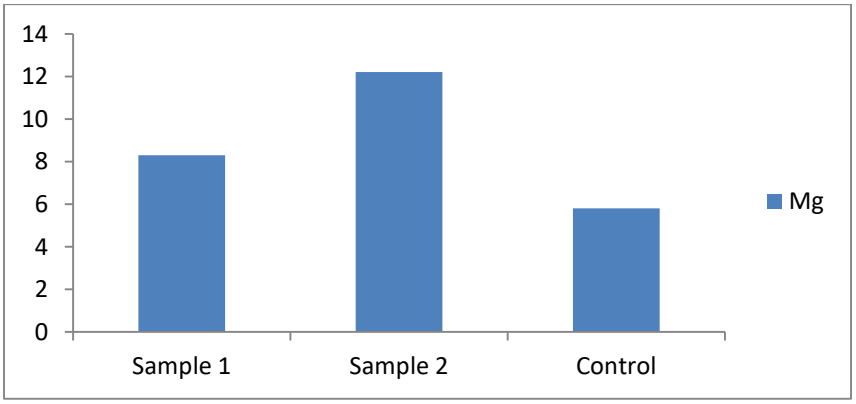

Fig.12: Plot of Mg against sampling points**.**

Sodium (Na)

Sodium present in drinking water may originate from various natural sources, such as mineral deposits found in the earth and sea spray. Additionally, it can be introduced through human activities, which include the application of road salt, the use of chemicals in water treatment, and the deployment of water softeners. Furthermore, sodium is naturally found in groundwater, particularly in regions close to coastal areas. The concentration of Na ranges from 5.4 to 10.4 mg/L, with an average value of 7.63 mg/L as shown in Table 1, and Fig.13. Deduction from the study revealed that Na for this study, is below permissible limit of 200 mg/L recommended by WHO, (2011).

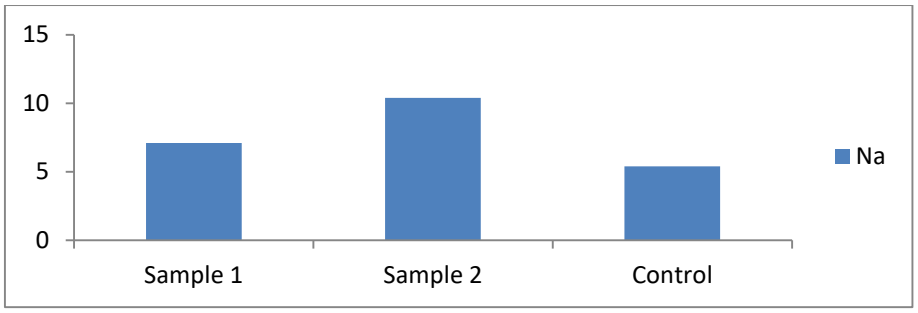

Fig. 13: Plot of Na against sampling points**.**

Potassium (K)

The presence of potassium in drinking water may originate from either natural sources or the processes involved in water treatment. Natural sources encompass the soil and rocks that water traverses, whereas water treatment may utilize chemicals that contain potassium, such as potassium permanganate or potassium chloride. The concentration of K for this study ranges from 8.3 to 14.9 mg/L, with average value of 11.27 mg/L see Table 1, and Fig. 14. Observation revealed that K value for this study is far below the permissible limit of 200 mg/L recommended by WHO, (2011). Groundwater within the sample area is consider fit for drinking.

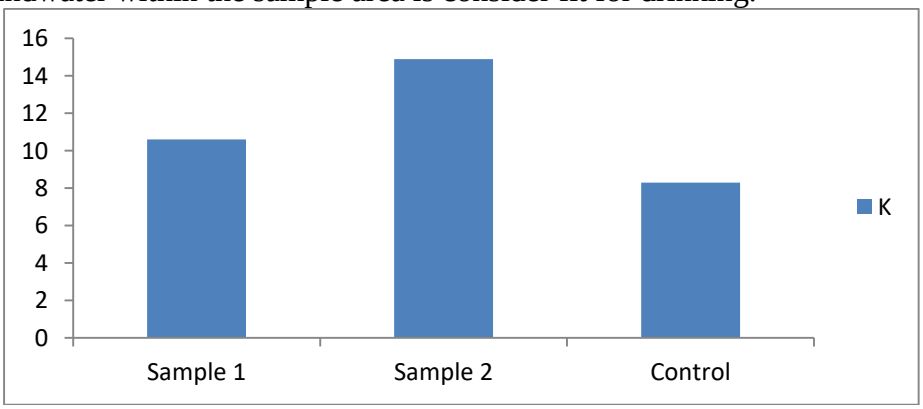

Fig. 14: Plot of K against sampling points**.**

Chloride (Cl^-)

The concentration of Cl for this study, ranges from 9.4 to 20.9 mg/L, with an average value of 15.57 mg/L as shown in Table 1, and Fig. 15. Findings from the study, showed Cl is below the permissible limit of 250 mg/L recommended by WHO, (2011). Chloride present in drinking water may originate from both natural processes and anthropogenic activities. The natural contributors encompass the erosion of soils and rocks, the presence of mineral deposits, and the infiltration of seawater in coastal regions. In contrast, human-induced sources consist of road de-icing salts, discharges from industrial and agricultural wastewater, as well as effluents from wastewater treatment facilities.

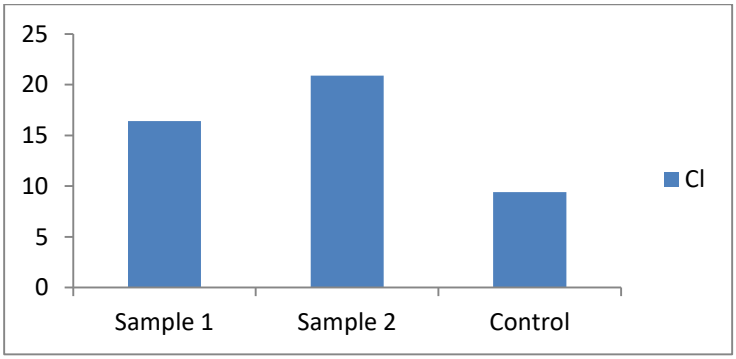

Fig. 15: Plot of Cl against sampling points.

Nitrate (NO_3^-)

NO_3^- contamination in drinking water can originate from a multitude of sources, such as farming practices, wastewater management, and industrial operations. A significant contributor is agricultural runoff, particularly that resulting from the excessive use of inorganic nitrogen fertilizers and animal manures. Furthermore, nitrate may enter water systems through effluents from wastewater treatment facilities and industrial activities. Moreover, septic systems, along with both human and animal waste, can introduce nitrate into both groundwater and surface water bodies (WHO, 2019). The concentration of NO_3^- ranges from 0.82 to 2.63 mg/L, with an average value of 2.22 mg/L as shown in Table 1, and Fig. 16.

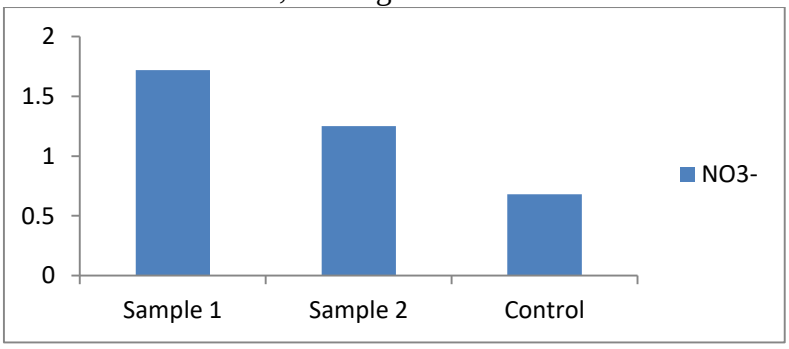

Fig. 16: Plot of Cl against sampling points.

Sulphate (SO_4^{2-})

The primary direct and indirect contributors to anthropogenic SO_4^{2-} input in aquatic systems include acid mine drainage, the leaching of fertilizers from agricultural lands, the drainage of wetlands, runoff from agricultural and industrial wastewater, and fluctuations in sea levels (Eyankware, et al., 2020; Onwe, et al., 2020). The concentration of SO_4^{2-} ranges from 0.68 to 1.72 mg/L, with an average value of 1.22 mg/L see Table 1, and Fig. 17. The average value of SO_4^{2-} is below the permissible limit of 200mg/L prescribed by WHO, (2011).

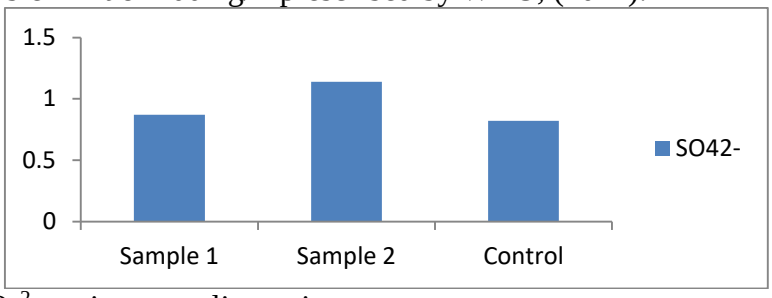

Fig. 17: Plot of SO_4^{2-} against sampling points.

Phosphate (PO_2^{4-})

Contamination of drinking water with phosphates can originate from both natural and anthropogenic sources. The natural contributors involve the weathering processes of rocks and minerals that are rich in phosphorus, runoff generated from agricultural fields, and the breakdown of organic materials. On the other hand, human activities, including the application of detergents, industrial waste discharges, runoff from agricultural practices, and effluents from wastewater treatment facilities, significantly elevate phosphate concentrations in drinking water. The concentration of PO_2^{4-} for this ranges 0.21 to 1.08 mg/L, with an average of 0.68 mg/L as shown as Table 1, and Fig. 18. The permissible threshold for phosphate in drinking water is established by the World Health Organization (WHO) at 1 mg/L. Research indicates that elevated levels of phosphate may be present in regions affected by agricultural activities or wastewater discharge. Deduction from the findings suggested that sample location 2 is above WHO, (2011) permissible limit. Hence sample location two is not considered suitable for drinking purpose

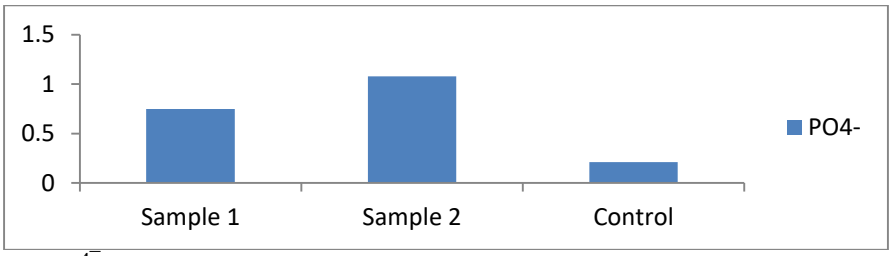

Fig. 18: Plot of PO_2^{4-} against sampling points.

NH4-N

Ammoniacal nitrogen (NH4–N) present in drinking water can originate from a range of both anthropogenic and natural sources. The natural sources primarily involve the decomposition of

organic materials, whereas significant contributions arise from human activities, especially those related to agriculture and wastewater management. The concentration of NH4-N ranges from 0.07 to 2.04 mg/L, with an average value of 1.25 mg/L as shown in Table 1, and Fig. 19. The WHO has established a maximum allowable concentration of 0.5 mg/l for drinking water. Nonetheless, it is common to detect NH4+ /NH3 concentrations exceeding 3 mg/L. The primary contributors to this pollution include the excessive application of fertilizers, overuse of livestock, urban wastewater, and contaminated discharges from industrial activities. Findings revealed that sample 2, is above WHO permissible limit.

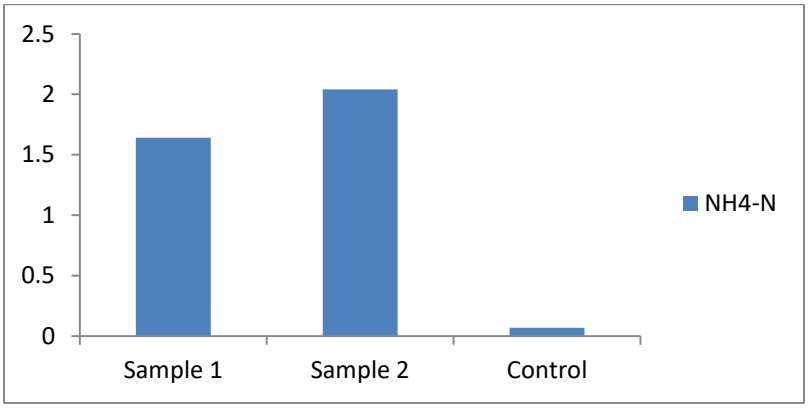

Fig. 19: Plot of NH4-N against sampling points.

Heavy Metal in groundwater within the study area

Iron (Fe)

The concentration of Fe for this study ranges from 0.02 to 0.14 mg/L, with an average value of 0.07 mg/L as shown in Table 1, and Fig. 20. The allowable threshold for lead in potable water is established at 0.01 mg/L (equivalent to10 µg/L). This maximum concentration is endorsed by the WHO as well as various other health institutions. The presence of iron in drinking water may originate from both natural phenomena and anthropogenic influences. Naturally, iron exists within the earth's crust and can leach into water as it traverses through soil and rock formations (Eyankware, et al., 2019). Furthermore, iron pipes, particularly those exhibiting signs of corrosion, may also release iron into the water supply. Deduction from Fig. 20, showed that the concentration of Fe for this study is above the recommended permissible limit. Eyankware, et al., (2023) were of the view that increase in concentration of Fe may originate from the degradation of iron or steel pipes, as well as other elements within the plumbing system, particularly when the water's acidity, indicated by a pH level, falls below 6.5.

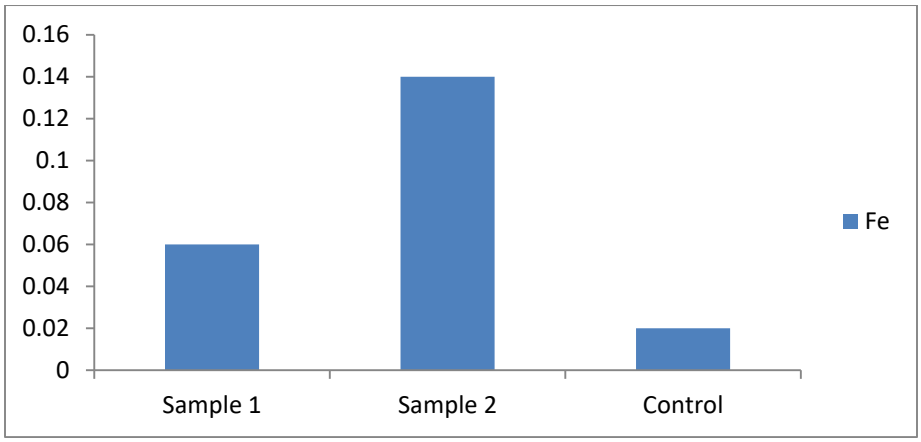

Fig. 20: Plot of NH4-N against sampling points.

Chromium (Cr)

Cr present in drinking water can originate from both natural and anthropogenic sources (Mahapatra et al., 2020). Natural origins encompass processes such as weathering and erosion of rocks and soils, whereas anthropogenic contributions primarily stem from industrial discharges, including those from steel and pulp mills, metal plating facilities, and various other industrial activities. The concentration of Cr for this study ranges from 0.008 to 0.021 mg/L, with an average value of 0.01 mg/L as shown in Table 1, and Fig. 21. The acceptable threshold for total Chromium concentration in drinking water is set at 0.05 mg/L, equivalent to 50 µg/L. The permissible limit of Cr is far below the threshold limit. Based on that groundwater is considered safe for drinking

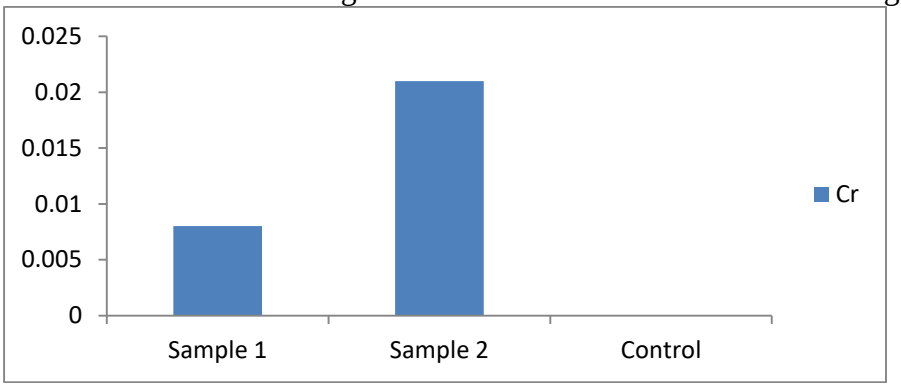

Fig. 21: Plot of Cr against sampling points

Lead (Pb)

The presence of lead in drinking water chiefly arises from the corrosion of plumbing materials that contain lead, such as pipes, faucets, and solder used in buildings and water systems (Eyankware, et al., 2022a). Additionally, the leaching of lead into the water may also result from parts of hand pumps or other substances that include lead or lead-stabilized PVC. The concentration of Pb were fall below the permissible limit see Table 1. According to the World Health Organization (WHO)

and numerous other entities, the acceptable threshold for lead concentration in drinking water is set at 0.01 mg/L, equivalent to10 µg/L.

Copper (Cu)

The main contributor of Cu in drinking water is the leaching process from copper pipes and fittings within plumbing infrastructures (Eyankware, et al. 2020). This leaching takes place when water interacts with copper components, especially during prolonged periods of stagnation. Additionally, copper may infiltrate the water supply via industrial effluents, wastewater from mining activities, and the natural erosion of rocks containing copper. The concentration of Cu for this study ranges from 0.011 to 0.05 mg/L, an average value of 0.03 mg/L as shown in Table 1, and Fig. 22. The concentration of Cu is below the permissible limit of 2mg/L recommended by WHO, (2011).

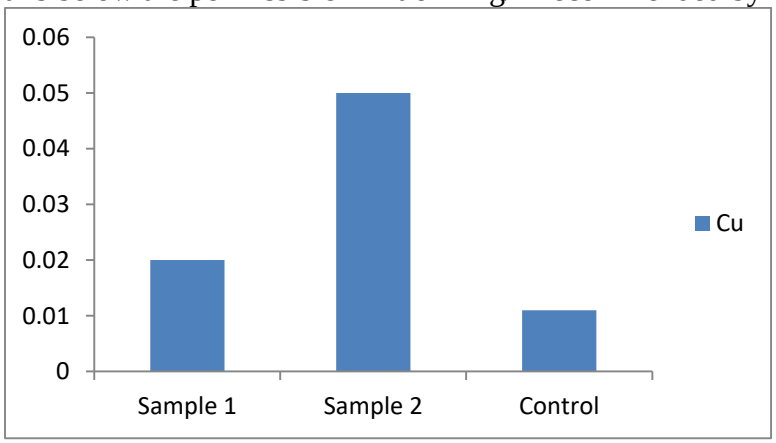

Fig.22: Plot of Cu against sampling points.

Zinc (Zn)

Zn may find its way into drinking water via both natural sources, such as minerals eroded from rocks and soil, and anthropogenic activities, including mining, steel manufacturing, and the utilization of galvanized pipes (Eyankware and Effam, 2019). Furthermore, the introduction of zinc compounds to water is often employed to prevent corrosion, while the deterioration of galvanized pipes or metal fixtures can further elevate zinc concentrations. The concentration of Zn for this study ranges from 0.014 to 0.08 mg/L, with an average value of 0.05 mg/L as shown in Table 1, and Fig.23. According to the EPA, the acceptable concentration of zinc in drinking water is typically regarded as 5.0 mg/L, equivalent to 5 ppm.

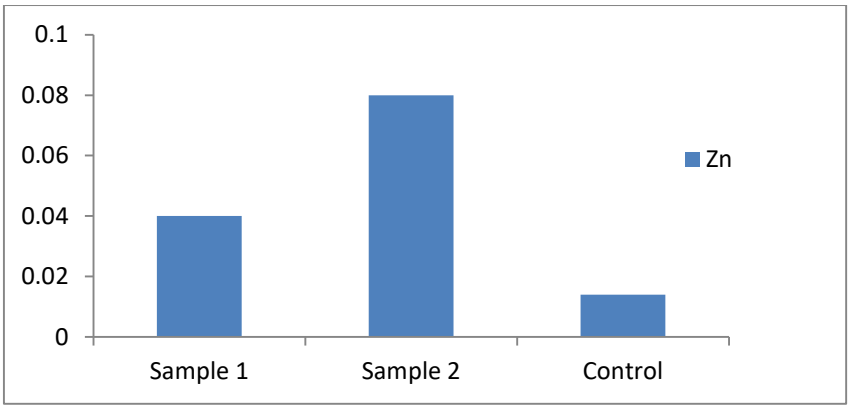

Fig. 23: Plot of Zn against sampling points

Nickel (Ni)

For this study the concentration of Ni is zero, the main source of nickel in drinking water is the leaching process from metals that are in contact with the water, especially those found in nickel or chromium-plated fixtures and internal plumbing systems (Eyankware, et al., 2020). Furthermore, nickel may also be present naturally in certain groundwater sources as a result of the dissolution of ore-containing rocks. It is probable that no definitive threshold exists for nickel (Ni) in groundwater. According to the WHO, (2019), the toxicity data pertaining to water-soluble nickel salts proves to be the most relevant in assessing the health risks associated with nickel exposure through drinking water. Following acute exposure to nickel, individuals may experience gastrointestinal and neurological symptoms, and sensitization to nickel can arise via dermal contact or inhalation. From Table 1, the value of Ni were below zero.

Manganese (Mn)

Mn present in drinking water may originate from both natural processes and anthropogenic actions. In nature, manganese is released from minerals found in soil and rock as water filters through these materials, subsequently infiltrating aquifers. Additionally, human endeavors such as mining operations, industrial waste discharges, and leaching from landfills can introduce manganese into water supplies. The concentration of Mn ranges from 0.013 to 0.022 mg/L, with an average value of 0.02 mg/L see Table 1, and Fig. 24.

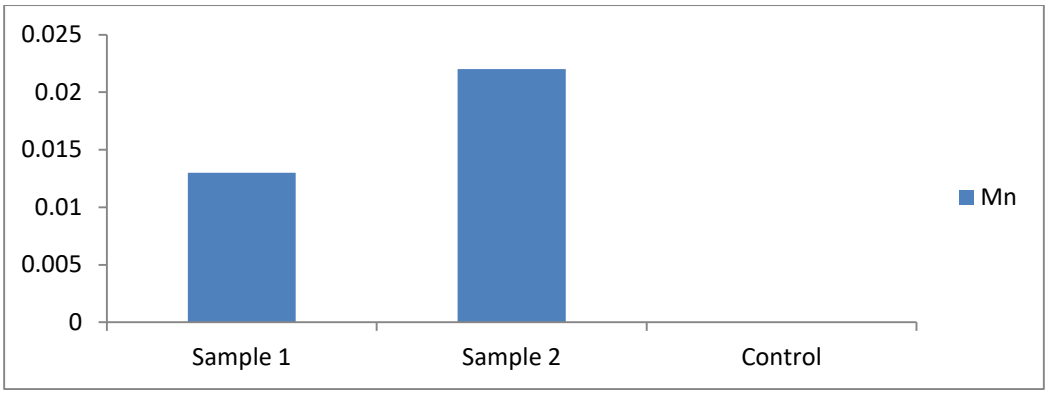

Fig. 24: Plot of Mn against sampling points

Cadmium (Cd)

The presence of cadmium in drinking water can be attributed to both natural and anthropogenic sources. On the natural side, cadmium may leach from soils and rocks, whereas human-related activities such as industrial operations, mining activities, and the incorporation of cadmium in numerous products play a significant role in its introduction. The occurrence of Cd was not found in groundwater within the study area see Table 1.

Assessment of Physicochemical in soil within the study area

pH

Soil pH, which indicates the level of acidity or alkalinity, results from a combination of natural processes and human activities. Major contributors to soil pH include the parent material, the effects of weathering, plant interactions, and anthropogenic influences. In particular, the characteristics of the soil's original rock (parent material) and the manner in which it undergoes weathering over time—shaped by climatic conditions and vegetation—greatly influence its pH level. Furthermore, the breakdown of organic matter, respiration from plant roots, and the use of specific fertilizers can also modify the pH of the soil. pH value for this study ranges from 5.28 to 7.20, with an average value of 6.17 see Table2, and Fig. 25.

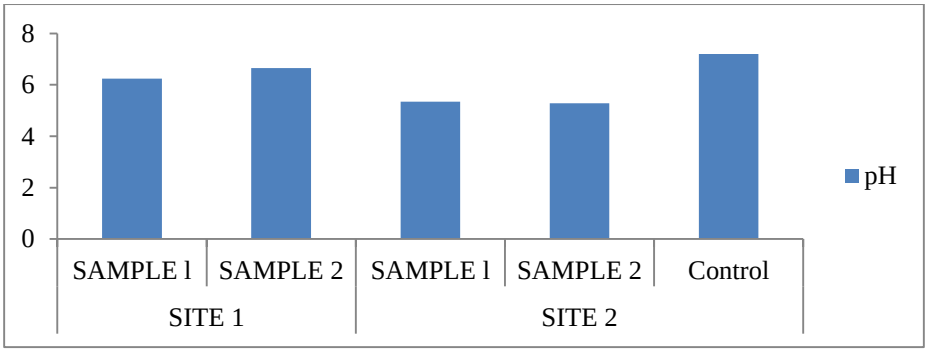

Fig. 25: Plot of pH against sampling points

Electrical Conductivity (EC)

Electrical conductivity in soils is predominantly due to the dissolved salts found within the soil water. These salts, which include ions such as calcium, magnesium, potassium, and sodium, possess electrical charges that facilitate the movement of current through the pores filled with water. The overall electrical conductivity of the soil is directly affected by both the amount of water present in the soil and the concentration of these dissolved salts. EC ranges from 101 to 165 µs/cm, with an average value of 137.4 µs/cm as shown in Table 2, and Fig. 26. The acceptable threshold for electrical conductivity (EC) in soil for the majority of plant species is typically regarded as being below 4 mS/cm (or 4 dS/m). An ideal EC range for promoting optimal growth in plants is generally between 0.2 and 0.8 dS/m, which provides adequate nutrients while minimizing salt stress. Furthermore, soils exhibiting an EC value between 3 and 4 mS/cm are still deemed suitable for a variety of plants.

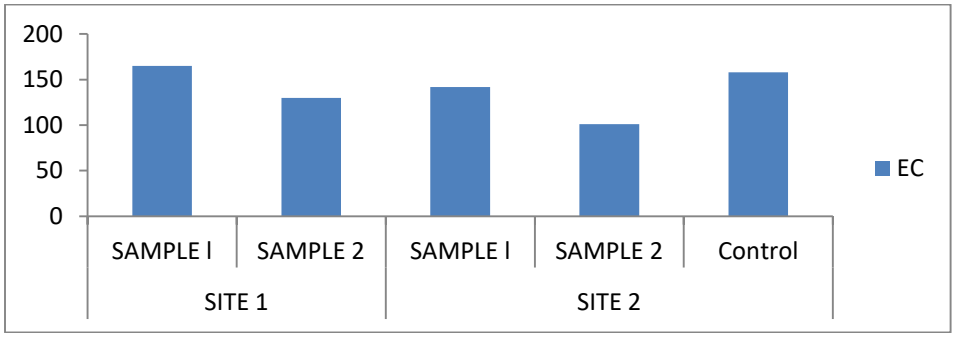

Fig.26: Plot of EC against sampling points

Alkalinity

Soil alkalinity, defined by a pH level exceeding 7, results from a multitude of both natural and anthropogenic factors, chiefly attributed to the existence of alkaline materials and the buildup of specific salts within the soil profile. The concentrations of soil alkalinity for this study ranges from 48.0 to 73.7, with an average value of 58.0 see Table 2, and Fig. 27

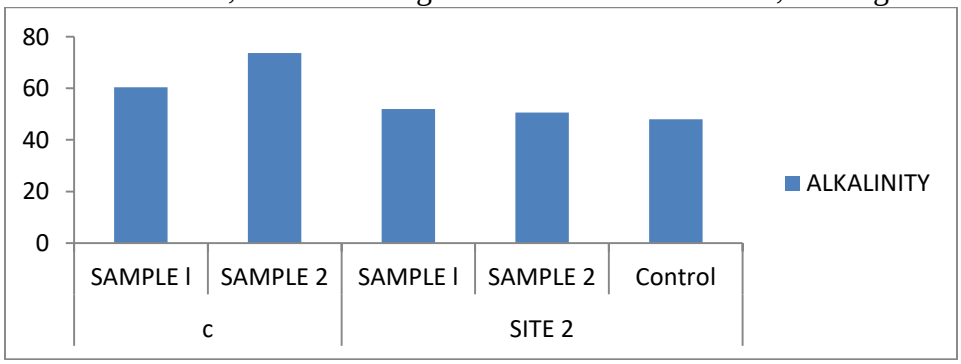

Fig. 27: Plot of alkalinity against sampling points

Calcium (Ca)

The primary source of calcium in soil is derived from a range of minerals, notably liming agents such as calcite and dolomite (Eyankware, et al., 2024). Furthermore, natural sources encompass minerals that contain calcium, including hornblende, mica, and feldspar. In addition to these natural sources, calcium can also be introduced into the soil through the application of fertilizers, which include lime, gypsum, and superphosphate. The concentration of Ca in soil ranges from 76 to 114 mk/kg, with an average value of 94.6 mk/kg as shown in Table 2, and Fig. 28. The average concentration of Ca is measured at 7.27 mg/kg, a figure that falls below the World Health Organization's permissible maximum range of 200 to 1300 mg/kg. Calcium present in soil can originate from a variety of both natural and synthetic sources. Among the natural sources are minerals such as limestone, dolomite, and gypsum. In contrast, applied sources typically consist of fertilizers including lime, gypsum, and calcium nitrate. Additionally, organic materials like crushed eggshells and bone meal play a role in enriching the soil with calcium.

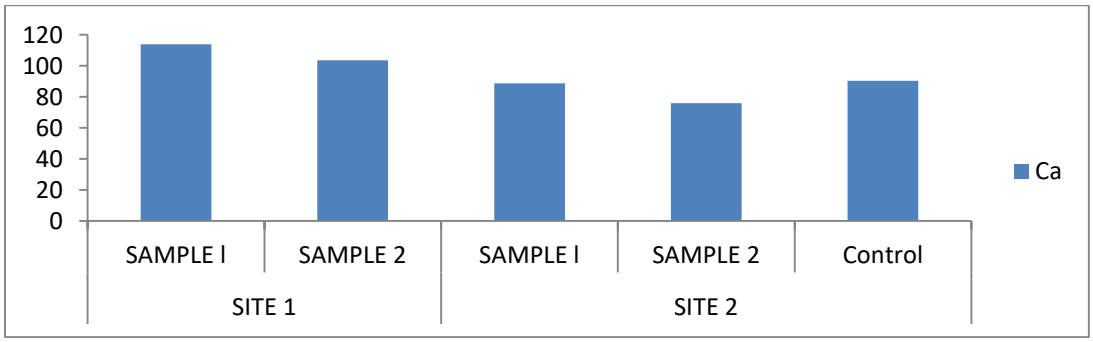

Fig.28: Plot of Ca against sampling points

Magnesium (Mg)

The presence of magnesium in soil can be attributed to multiple sources, such as the weathering of minerals, the application of fertilizers, and the use of irrigation water. The principal contributors to magnesium levels include primary silicate minerals such as olivine, serpentine, and dolomite. Furthermore, magnesium may also be supplemented through the use of fertilizers, animal manure, biosolids, and irrigation water. For this study, the concentration of Mg ranges from 44.7 to 121.8 mk/kg, with an average value of 84.2 mk/kg as shown in Table 2, Fig. 29.

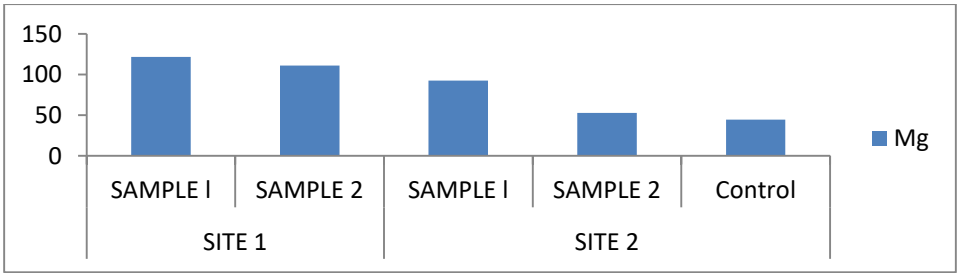

Fig.29: Plot of Mg against sampling points

Sodium (Na)

According to Eyankware, et al., (2024), the presence of sodium in soil can be attributed to a range of sources, encompassing both natural phenomena and anthropogenic activities. Among the natural sources are the weathering processes of sodium-rich minerals and the inherent sodium found in parent materials or groundwater. Additionally, human practices such as irrigation, excessive grazing, and the application of fertilizers and pesticides significantly elevate sodium concentrations in the soil. The concentration of Na ranges from 20 to 53.6 mk/kg, with an average value of 38.17 mk/kg as shown in Table 2, and Fig. 30.

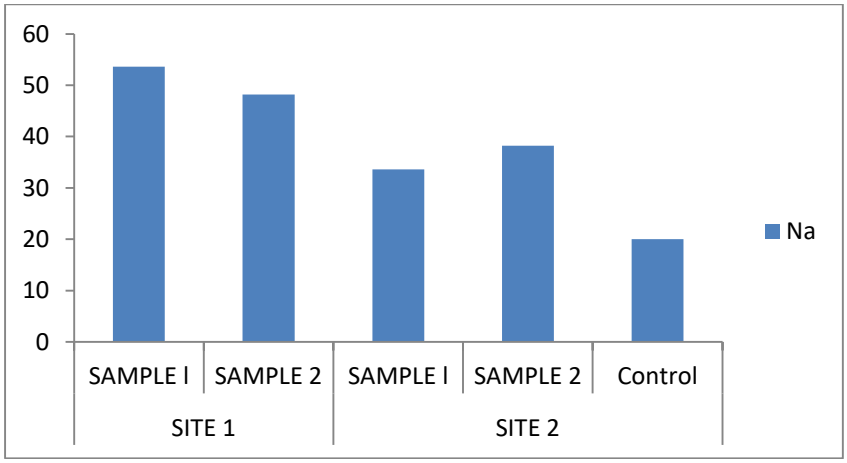

Fig. 30: Plot of Na against sampling points

Potassium (K)

The potassium present in soil originates from the natural weathering processes of rocks and minerals, in addition to the incorporation of both organic and inorganic substances. Major natural contributors include minerals such as feldspars and micas, which gradually decompose to liberate potassium. Furthermore, organic materials like compost, manure, and wood ash also enhance the potassium content of the soil. The concentration of K for this study ranges from 23.8 to 56 mk/kg, with an average value of 40.8 mk/kg as shown in Table 2, and Fig. 31. The WHO acceptable limit of ≤100 (ppm)

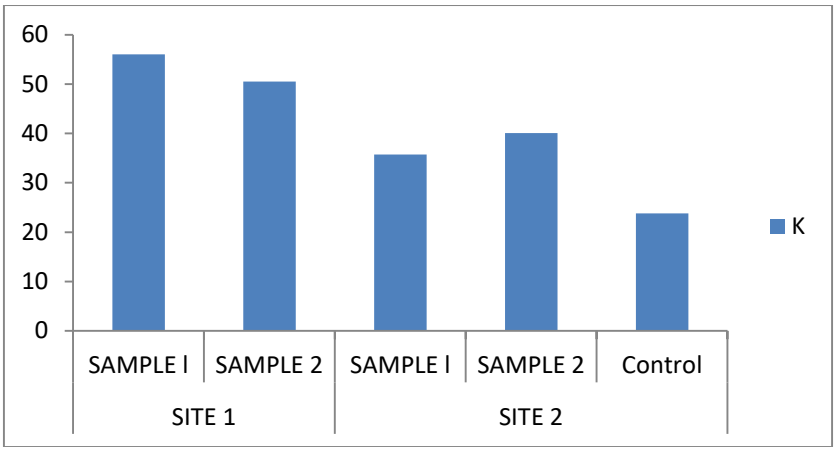

Fig. 31: Plot of K against sampling points

Chloride (Cl^-)

The introduction of chlorine into soils primarily results from the deposition of Cl through various sources, including rainwater, the application of fertilizers (such as KC1), irrigation water, sea spray, airborne dust, and pollution. The concentration of Cl^- in rainwater is influenced by its distance from saltwater bodies and exhibits significant variability. The concentration of Cl^- for this study ranges from 23.8 to 38.2 mk/kg, with an average value of 30.3 mk/kg as shown in Table 2, and Fig.32.

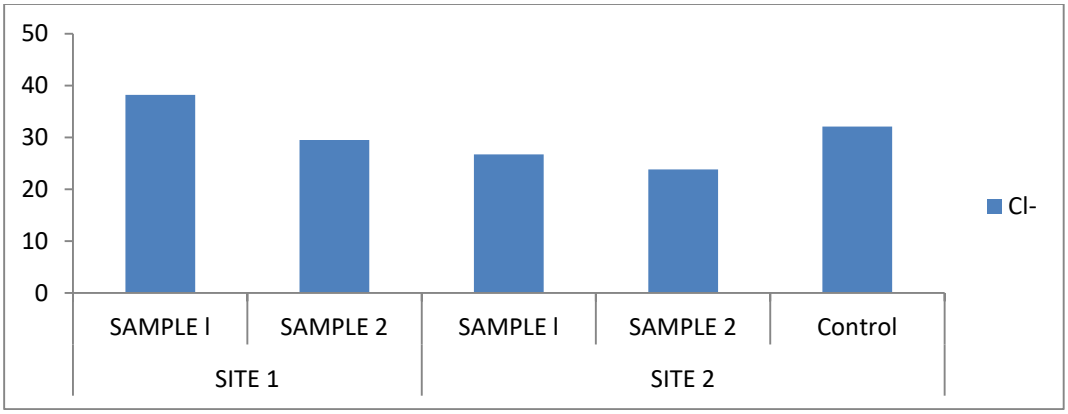

Fig. 32: Plot of Cl against sampling points

Sulphate (SO_2^{4-})

SO_2^{4-} present in soil is derived from a combination of natural and human-induced sources. The natural contributions include the weathering of geological parent materials, atmospheric deposition through both wet and dry processes, as well as the breakdown of organic matter. Additionally, anthropogenic activities, such as the disposal of industrial waste and the combustion of fossil fuels, play a substantial role in increasing atmospheric sulfate levels, which subsequently

settle onto the soil. The concentration of SO_2^{4-} for this study ranges from 0.75 to 4.8 mk/kg, with an average value of 2.52 mk/kg as shown in Table 2, and Fig. 33 The allowable concentration of sulfate in soil is contingent upon the specific context and intended use. Typically, a level of 0.2% or 224.4 ppm by weight of soil is regarded as non-toxic and negligible for construction applications.

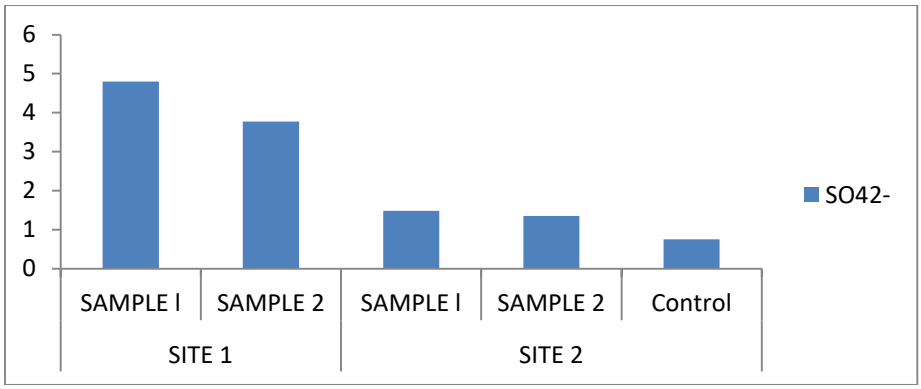

Fig. 33: Plot of SO4 against sampling points

Assessment of heavy metals in soil within the study area

Iron (Fe)

The concentration of Fe in soil for this study ranges from 38.2 to 123.8 mk/kg, with an average value of 87.0 mk/kg see Table 2, and, Fig. 34. The presence of iron in soil is mainly a result of the weathering processes affecting iron-rich minerals found within rocks, alongside contributions from organic matter (Eyankware, et al., 2025). The minerals involved encompass fundamental silicate varieties such as pyroxenes, amphiboles, and micas, in addition to iron oxides and hydroxides. Furthermore, organic matter, particularly when it has undergone decomposition by microorganisms, liberates iron in forms that are accessible for absorption by plants. The WHO, (2011) sets a recommended maximum threshold of 50,000 mg/kg for iron content in soil. Nevertheless, various studies propose more conservative limits, including values as low as 5,000 mg/kg. Levels that surpass these thresholds may signal potential contamination or toxicity in certain plant species, particularly in the case of rice. Further findings suggested that the Fe in soil is below the set limit.

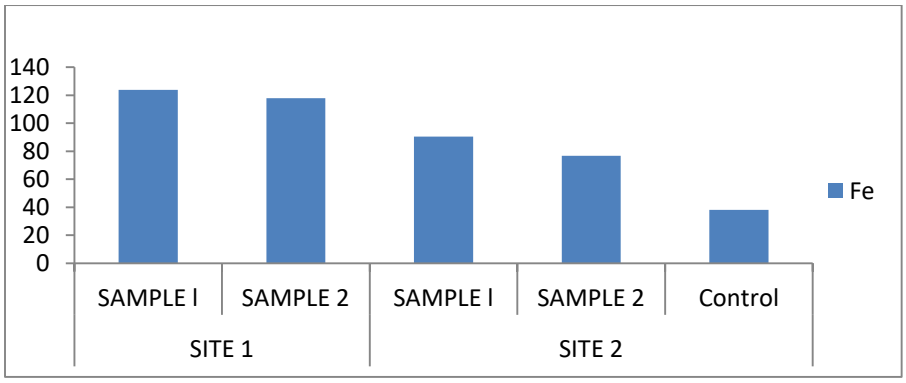

Fig. 34: Plot of Fe against sampling points

Lead (Pb)

Lead present in soil can arise from both natural processes and human endeavors. In its natural state, lead is a component of the Earth's crust, commonly found within various rocks and minerals. Human-related sources encompass lead-containing paints, leaded gasoline, emissions from industrial activities, and the recycling of lead-acid batteries. The concentration of Pb in soil ranges from 3.8 to 8.7 mk/kg, with an average value of 6.18 mk/kg as shown in Table 2, and Fig. 35

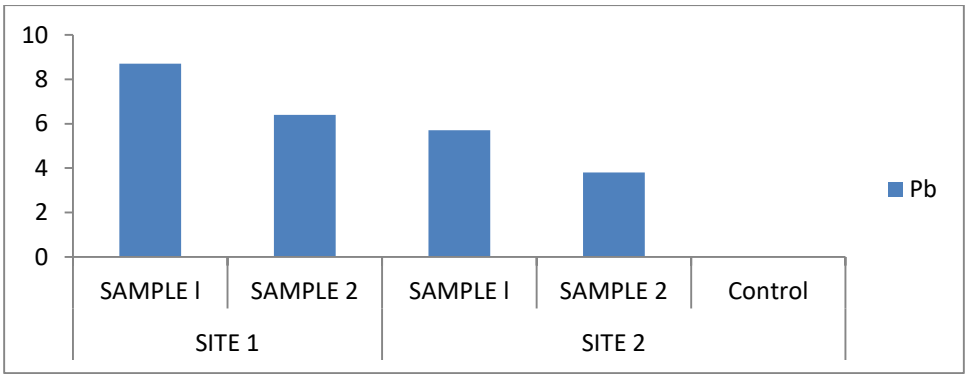

Fig.35: Plot of Pb against sampling points

Copper (Cu)

Cu present in soil can stem from both natural phenomena and human-induced actions. From a natural perspective, copper is introduced into the soil via the weathering of rocks, especially igneous and sedimentary types, as well as from mineral deposits. In contrast, human activities contribute copper through diverse agricultural methods, industrial operations, and the disposal of waste. The WHO permissible limit for copper in soil is 36 mg/kg. The concentrations of Cu for this study ranges from 3.8 to 34.5 mk/kg, with an average value of 20.15 mk/kg as shown in Table 2, and Fig.36 , further findings revealed that the concentration of Cu is below the set limit

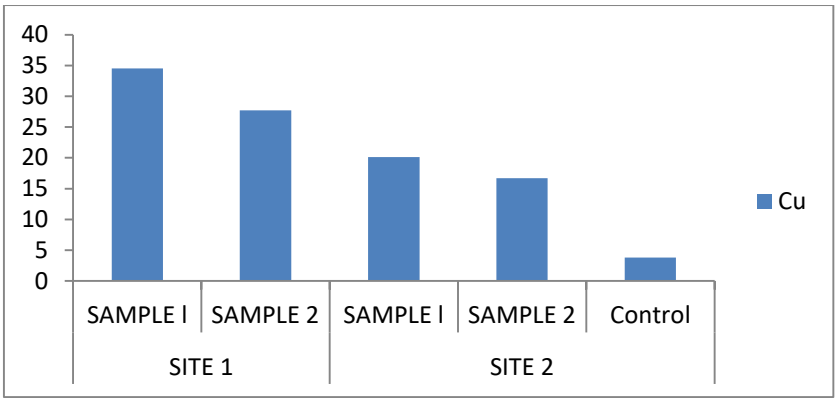

Fig. 36: Plot of Pb against sampling points**:**

Chromium (Cr)

Cr present in soil originates from a combination of natural and anthropogenic sources (Igwe, et al., 2021). The natural sources encompass continental dust and the weathering processes of rocks that contain chromium minerals. On the other hand, anthropogenic sources, which are linked to human activities, consist of emissions from industrial operations, inadequate disposal of both industrial and municipal waste, as well as the application of products that contain chromium in agricultural practices. The permissible limit of Cr in soil typically fluctuates based on the relevant regulatory body and the intended application of the soil. Nevertheless, the World Health Organization/Food and Agriculture Organization (WHO/FAO) establishes a permissible threshold of 50 mg/kg (parts per million) for Cr content in soil. Findings from Table 2, and Fig. 37, showed that the Cr value for this study ranges from 2.88 to 18.6 mk/kg, with an average value of 10.16 mk/kg. The aforementioned values were below the recommended threshold value

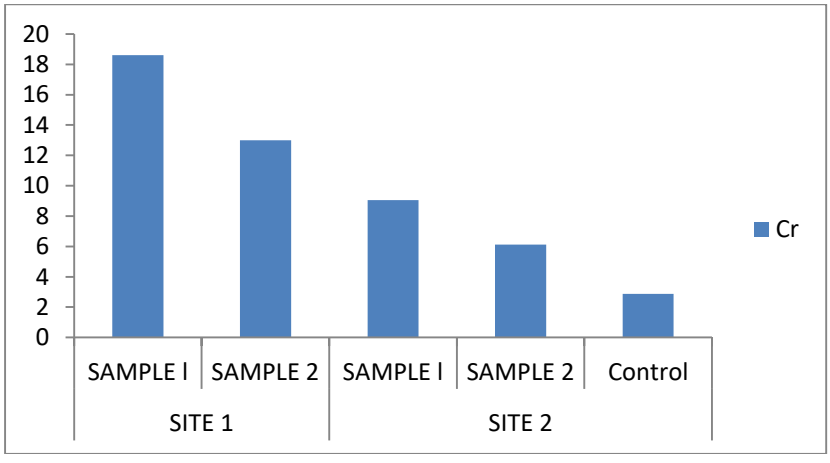

Fig. 37: Plot of Cr against sampling points

Zinc (Zn)

The presence of zinc in soil can be attributed to both natural (geogenic) and human-induced (anthropogenic) factors. Zinc naturally occurs within the Earth's crust and various rock formations, with its levels in soil being affected by the soil's parent material. Human activities contributing to Zn levels include mining and smelting processes, the disposal of industrial waste, and agricultural methods such as the use of fertilizers and the application of sewage sludge. The acceptable concentration of zinc in soil typically ranges from 300 to 400 mg/kg (milligrams per kilogram). The WHO and the FAO, have established a threshold of 300 mg/kg as the permissible limit. Furthermore, in soils with acidic properties, a DTPA-extractable zinc level exceeding 10 mg/kg is regarded as potentially detrimental. From Table 2, and Fig. 38. It was noticed that the value of Zn ranges from 4.1 to 43.9 mk/kg, with an average value of 24.17 mk/kg. That implies that the concentration of Zn for this study is below WHO and the FAO are set limit.

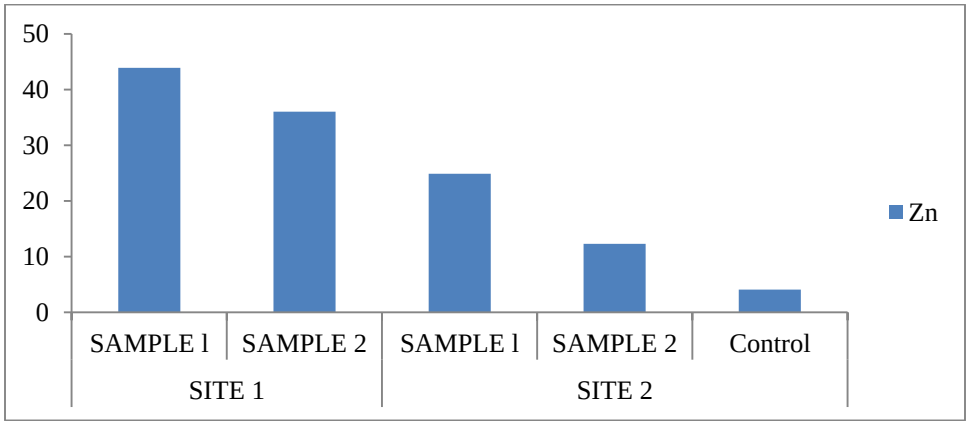

Fig. 38: Plot of Zn against sampling points

Nickel (Ni)

Nickel present in soil can arise from both natural and human-made sources. In nature, nickel occurs in a variety of minerals such as pentlandite, garnierite, and other ores that contain nickel. In terms of human influence, sources include industrial waste, activities related to mining and smelting, the application of sewage sludge and phosphate fertilizers, as well as atmospheric deposition resulting from emissions, particularly those associated with fossil fuel combustion. The acceptable concentration of Ni in soil typically ranges from 35 to 150 mg/kg, equivalent to 35-150 ppm (WHO, 2011). Observation from Table 2, and Fig. 39, revealed that Ni ranges from 3.08 to 4.92 mk/kg, with an average value of 4.33 mk/kg, that implies that Ni is below the permissible limit.

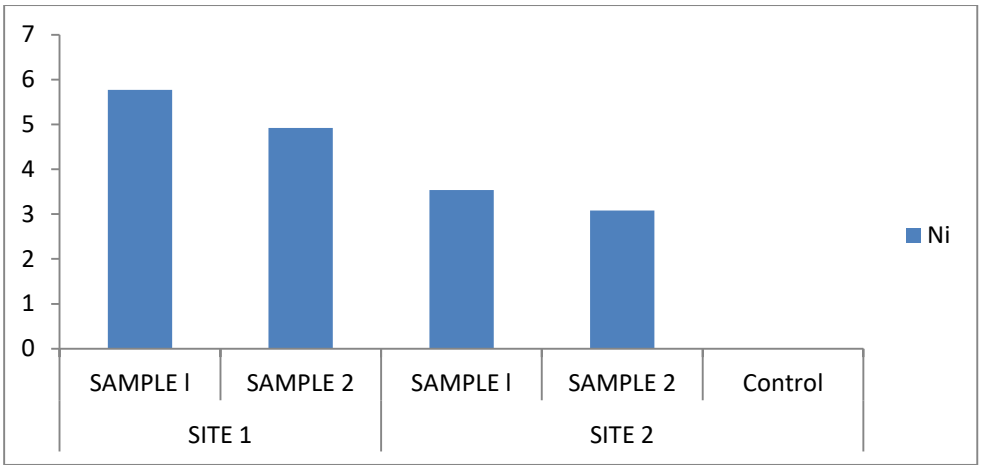

Fig.39: Plot of Ni against sampling points

Discussion on Time lapse

Time Lapse of Presco upland

Comprehensive analyses of the soil and water indicated that both sites are influenced by a plume of fertilizer contaminants. The leachate plumes from fertilizers were identified in the initial site (Presco lowland), and a time lapse study was subsequently conducted to verify the findings from the 2023 ERT survey. The resistivity measurements obtained during the 2024 survey across several lines ranged from 109 Ωm to 2862 Ωm, aligning with the interpretations made in 2023. Furthermore, the time lapse study conducted at the first site (Presco lowland) to observe the movement of contaminant plumes demonstrated that the highest rate of vertical contaminant migration within the subsurface reached 216.7 cm/month, while the horizontal migration rate was recorded at 750.0 cm/month. A time lapse investigation of the second site (Presco upland) conducted to observe the movement of contaminant plumes reveals that the highest rate of vertical contaminant migration within the subsurface at this location is 122.5 cm/month, whereas the horizontal migration rate reaches 500.0 cm/month. These findings indicate that both study locations remain significantly active at the time of this assessment. Detailed computations of the migration rates can be found in Table 3 and Table 4.

Table 3: Result of Time lapse study of the Presco Lowland

PLUME TRAVERSE NO.	Date	Vertical Position (m)	Horizontal Position (m)	Vertical Migration (m)	Horizontal Migration (m)	Vertical Migration Rate (cm/month)	Horizontal Migration Rate (cm/month)
ERT1	6/08/14	2.8	8.0	10.0	22.0	83.3	183.3
	11/08/15	12.8	30.0				
ERT3	6/08/14	12.8	90.0	26.8	10.0	216.7	83.3
	11/08/15	39.6	80.0				
ERT6	6/08/14	39.6	75.0	21.1	15.0	175.8	125.0
	11/08/15	18.5	90.0				
ERT7	6/08/14	24.9	95.0	14.7	50.0	122.5	416.7
	11/08/15	39.6	40.0				
ERT8	6/08/14	18.5	120.0	6.4	80		
	11/08/15	24.9	40.0			53.3	666.7
ERT9	6/08/14	19.8	22.0	13.4	78.0	111.7	650.0
	11/08/15	6.38	100.0				
ERT11	6/08/14	19.8	80.0	3.9	10.0	32.5	83.3
	11/08/15	15.9	90.0				
ERT13	6/08/14	6.38	10.0	13.4	90	111.7	750
	11/08/15	19.8	100.0				

Table 4: Result of Time lapse study of the Presco Upland

Plume No.	Date	Vertical Position (m)	Horizontal Position (m)	Vertical Migration (m)	Horizontal Migration (m)	Vertical Migration Rate (cm/month)	Horizontal Migration Rate (cm/month)
ERT17	5/08/2014	31.9	80.0	7.7	60.0	64.2	500.0
	10/08/2015	39.6	140.0				
ERT18	5/08/2014	24.9	200.0	14.7	40.0	122.5	333.3
	10/08/2015	39.6	160.0				
ERT21	5/08/2014	24.9	180.0	14.7	20.0	122.5	166.7
	10/08/2015	39.6	200.0				

A subsequent ERT survey was carried out precisely one year later, in April 2024, at which point it is likely that the fertilizer contaminant plumes had either been diluted due to the influx of excess infiltrating water or had experienced additional fertilizer leachate, thereby facilitating a more rapid movement both vertically and horizontally. The migration rate is influenced by the soil's porosity and permeability, as well as the surrounding topography. Notably, the rates of migration observed at the first and second locations exhibit distinct differences. It has been determined that, assuming a constant vertical migration rate within the dry sand layer—averaging approximately 13.7 meters

based on borehole drilling data—it would take roughly 0.5 years and 1 year for the fertilizer contaminants plume to reach the saturated sandy layer directly beneath it at the first and second locations, respectively. The specifics of the calculations regarding the arrival time at the sandy layer are detailed in Table 5. Furthermore, it is evident that the horizontal migration rate surpasses the vertical migration rate, with differences of 133.4 cm/month and 210.8 cm/month observed in the second and third cemeteries, respectively.

Table 5: Migrating plume arrival time in subsoil in the different locations

Location	Maximum vertical migration rate(m/month)	Surface layer average thickness(m)	Predicted arrival time in the underlying sandy soil (years)
First location (Presco Lowland)	2.167	13.7	0.5
Second Location (Presco Upland)	1.225	13.7	1

Time Lapse of Presco lowland

The fertilizer leachate plumes were located in the first location (Presco lowland), a time lapse study in ERT survey. The resistivity recorded for the 2024 survey on some survey lines varied from 109 Ωm to 2862 Ωm. A time lapse study of the first location (Presco lowland) to monitor the migration of contaminants plumes shows that the maximum rate of contaminant migration within the subsurface in the vertical direction in the first location is 216.7 cm/month, while the horizontal migration rate is750.0 cm/month respectively. While a time lapse study of the second location (Presco upland) to monitor the migration of contaminants plumes shows that the maximum rate of contaminant migration within the subsurface in the vertical direction in the second location is 122.5 cm/month, while the horizontal migration rate is 500.0 cm/month respectively. These results show the status of the study locations: the first and the second location much still active as at the time of this survey. Table 6 and Table 7 give the details of the computation of migration rates.

Table 6: Result of Time lapse study of the Pesco Lowland

PLUME TRAVERSE NO.	Date	Vertical Position (m)	Horizontal Position (m)	Vertical Migration (m)	Horizontal Migration (m)	Vertical Migration Rate (cm/month)	Horizontal Migration Rate (cm/month)
ERT1	6/08/14	2.8	8.0	10.0	22.0	83.3	183.3
	11/08/15	12.8	30.0				
ERT3	6/08/14	12.8	90.0	26.8	10.0	216.7	83.3
	11/08/15	39.6	80.0				
ERT6	6/08/14	39.6	75.0	21.1	15.0	175.8	125.0
	11/08/15	18.5	90.0				
ERT7	6/08/14	24.9	95.0	14.7	50.0	122.5	416.7
	11/08/15	39.6	40.0				
ERT8	6/08/14	18.5	120.0	6.4	80		
	11/08/15	24.9	40.0			53.3	666.7
ERT9	6/08/14	19.8	22.0	13.4	78.0	111.7	650.0
	11/08/15	6.38	100.0				
ERT11	6/08/14	19.8	80.0	3.9	10.0	32.5	83.3
	11/08/15	15.9	90.0				
ERT13	6/08/14	6.38	10.0	13.4	90	111.7	750
	11/08/15	19.8	100.0				

Table 7: Result of Time lapse study of the Presco Upland

Plume No.	Date	Vertical Position (m)	Horizontal Position (m)	Vertical Migration (m)	Horizontal Migration (m)	Vertical Migration Rate (cm/month)	Horizontal Migration Rate (cm/month)
ERT17	5/08/2014	31.9	80.0	7.7	60.0	64.2	500.0
	10/08/2015	39.6	140.0				
ERT18	5/08/2014	24.9	200.0	14.7	40.0	122.5	333.3
	10/08/2015	39.6	160.0				
ERT21	5/08/2014	24.9	180.0	14.7	20.0	122.5	166.7
	10/08/2015	39.6	200.0				

The first ERT survey was conducted in April 2023 and fertilizer contaminant plumes were delineated. The second ERT survey was executed exactly 12 months later, in April 2024, when the fertilizer contaminate plumes must have been diluted with excess infiltrating water or more fertilizer leachate added and so move faster in the vertical and horizontal directions. The rate of migration depends on the porosity and permeability of the soil and topography. The migration rates are distinctive in the first and second location. However, it is revealed that if the vertical migration rate is constant in the dry sand layer (average thickness of about 13.7m from borehole drilling

information), then it will take about 0.5and 1 years for the fertilizer contaminants plume in the first and second location respectively to arrive at the saturated sandy layer just below it. Table 7 shows the detail of the computation of arrival time to the sandy layer. Moreso, it is also seen that the rate of migration in the horizontal direction is higher than that in the vertical direction by margins of 133.4 cm/month and 210.8 cm/month and in the second and third cemeteries respectively.

Table 7: Migrating plume arrival time in subsoil in the different locations

Location	Maximum vertical migration rate(m/month)	Surface layer average thickness(m)	Predicted arrival time in the underlying sandy soil (years)
First location (Presco Lowland)	2.167	13.7	0.5
Second Location (Presco Upland)	1.225	13.7	1

CONCLUSION

This study carried out assessment of water and soil impacted by application of fertilizer within study area for physicochemical, and heavy metals concentration. A total of three (3) groundwater sample was carried out within the study area, one ot of the three sample was used as control site. As for soil a total of four (4) , two (2) each from each sample site. In the study presented, time-lapse geophysical measurement using ERT was used to analyze the impact of fertilization on the measured geophysical signals. Analysis of the groundwater and soil indicated that the groundwater samples fell below the permissible limits set by the WHO, with the exception of a few parameters. The migration rate is influenced by the soil's porosity and permeability as well as the topographical features. Notably, the migration rates differ between the first and second locations. It has been determined that, assuming a consistent vertical migration rate within the dry sand layer (approximately 13.7 m thick based on borehole drilling data), the fertilizer contaminants plume will reach the saturated sandy layer beneath in approximately 0.5 years at the first location and 1 year at the second location. Detailed calculations regarding the arrival time to the sandy layer.

REFERENCES

Adeyeye, J. A., Akinyemi, O. D., Awomeso, J. A., Bada, B. S., Akintan, O. B. (2021). Geo-chemical investigation of groundwater salinity status in selected coastal areas of south

western Nigeria. Sustain Water Res Manag. https://doi.org/10.1007/s40899-021-00541-9

Akinseye, V.O., Osisanya, W.O., Eyankware. M. O., Korode, I.A.., Ibitoye, A.T. (2023). Application of second-order geoelectric indices in determination of groundwater vulnerability in hard rock terrain in SW. Nigeria. Sustainable Water Resources Management. 9:169, https://doi.org/10.1007/s40899-023-00936-w

Chandrasekar N, Selvakumar S, Srinivas Y et al (2013) Hydro-geochemical assessment of groundwater quality along the coastal aquifers of southern Tamil Nadu, India. Environ Earth Sci 71(11):4739–4750. https://doi.org/10.1007/s12665-013-2864-3

Eyankware. M. O., Effam, S. C. (2019). A preliminary assessment of hydrogeochemical quality of groundwater around rural communities of abandoned Nkalagu limestone quarry. SE Nigeria. Annals of Chemical Science Research, doi: 10.31031/ACSR.2019.01.000522

Eyankware, M. O., Igwe, E. O., Ulakpa, R.O.E., Ogwah, C. (2020a). Achieving sustainable use and management of water resources for irrigation in Nigeria-Review. Journal of Environmental & Earth Sciences, 2(2): 47-55.

Eyankware. M. O., Ogwah, C., Ulakpa. R.O.E. (2020b). The study of sea water intrusion in coastal aquifer of Niger Delta Region, Nigeria. Middle-East Journal of Scientific Research, 28(4): 369-379.

Eyankware., M. O., Ephraim, B. E. (2021). A comprehensive review of water quality monitoring and assessment in Delta State, Southern Part of Nigeria. Journal of Environmental and Earth Sciences. 3(1); 16-28.

DOI:https://doi.org/10.30564/jees.v3i1.2900.

Eyankware. M. O., Obasi, P. N. (2021). A holistic review of heavy metals in water and soil in Ebonyi SE. Nigeria; with emphasis on its effects on human, aquatic organisms and plants. World News of Natural Science, 38; 1-19.

Eyankware. M. O., Akakuru, C. O., Ulakpa, R. O. E., Eyankware, E.O. (2022a). Hydrogeochemical approach in the assessment of coastal aquifer for domestic, industrial, and agricultural utilities in Port Harcourt urban, southern Nigeria. International Journal of Energy and Water Resources. https://doi.org/10.1007/s42108-022-00184-2,

Eyankware. M. O., Akakuru, C. O., Eyankware, E.O. (2022b). Hydrogeophysical delineation of aquifer vulnerability in parts of Nkalagu areas of Abakaliki, SE. Nigeria. Sustainable Water Resources Management, https://doi.org/10.1007/s40899-022-00603-6.

Eyankware, M. O., Akakuru, O. C., Inoni, O. E., Osisanya, W. O., Ukor, K. P., Umuokoro, G. (2025). Interpretation of hydrochemical data in selected parts of Warri, Southern Nigeria using health risk assessment and heavy metal index. *Discovery Nature*; 2: e6dn3107doi: https://doi.org/10.54905/disssi.v2i3.e6dn3107

Igwe, E. O., Ede, C. O., Eyankware. M. O. (2021). Heavy metals concentration and distribution in soils around Oshiri and Ishiagu lead – zinc mining areas, southeastern Nigeria. World Scientific News. 158; 22-58.

Mahapatra, S. R., Venugopal, T., Shanmugasundaram, A., Giridharan, L., Jayaprakash, M. (2020). Heavy metal index and geographical information system (GIS) approach to study HM contamination: a case study of north Chennai groundwater. Appl Water Sci 10:238. https://doi.org/10.1007/s13201-020-01321-0

NSDWQ (2007) Nigerian standard for drinking water quality. Committee on Drinking Water Quality in Nigeria.

Onwe, I. M., Eyankware. M. O., Obasi, P. N., Ifeanyichukwu, K. A. (2022). Hydrochemical and statistical approaches in the evaluation of groundwater quality for drinking and irrigation uses around Ezzangbo–Ngbo area, Southeastern Nigeria. Modeling Earth Systems and Environment, https://doi.org/10.1007/s40808-022-01503-6.

Onwe, I. A. Obasi, Eyankware, M. O., Uchenna, O. L. (2024). An integration of hydrochemical data and stable isotopes in groundwater evaluation in Ngboejogu, Southern Benue Trough, Nigeria. Modeling Earth Systems and Environment https://doi.org/10.1007/s40808-024-02166-1.

Oseji, O. T., Egbai, J.C., Emuobonuvie, I. A. (2020). Aquifer vulnerability using geophysical and physiochemical methods in parts of Ethiope West Local Government Area of Delta State, Nigeria. *Advances* 10, 085209 (2020)
https://doi.org/10.1063/5.0015357

World Health Organization (WHO) (2011) Guidelines for drinking water quality, 4th edn. NLM classifcation: WA 675, World Health Organization, Geneva, Switzerland, pp 307–43

WHO (World Health Organization) (2019). Nickel in drinking-water draft background document for development of WHO guidelines for drinking-water quality.